The GAB2 signaling scaffold promotes anchorage independence and drives a transcriptional response associated with metastatic progression of breast cancer.

A. Mira,C. Isella,T. Renzulli,D. Cantarella,M. L. Martelli,E. Medico
The GAB2 signaling scaffold promotes anchorage independence and drives a transcriptional response associated with metastatic progression of breast cancer.
ONCOGENE (2009) 28
DOI: 10.1038/onc.2009.296

The GAB2 signaling scaffold promotes anchorage independence and drives a transcriptional response associated to metastatic progression of breast cancer.

Alessia Mira, PhD*, Claudio Isella, PhD*, Tommaso Renzulli, Dr, Daniela Cantarella, Dr. Maria Luisa Martelli, Dr, and Enzo Medico, MD PhD[1]

Laboratory of Functional Genomics, the Oncogenomics Center, Institute for Cancer Research and Treatment (IRCC), University of Turin Medical School, Str. Prov. 142, 10060 Candiolo, Italy.

Running Title: Gab2 promotes anchorage-independent growth.

*These authors contributed equally to the work

[1]Correspondence and reprint requests should be sent to: Enzo Medico, Institute for Cancer Research and Treatment, S.P. 142, km 3.95 - 10060 Candiolo (TO) Italy. Phone: +39-011-9933234 Fax: +39-011.9933225 E.mail: enzo.medico@ircc.it

Financial Support: This research was supported by grants from AIRC, the EC (contract n. 503438 “TRANSFOG”), CNR-MIUR, FIRB-MIUR, Ministero della Salute, Regione Piemonte and the Foundations CRT and ‘Compagnia di San Paolo’.

Abstract

Acquisition of independence from anchorage to the extracellular matrix is a critical event for onset and progression of solid cancers. To identify and characterize new genes conferring anchorage independence, we transduced MCF10A human normal breast cells with a retroviral cDNA expression library and selected them by growth in suspension. Microarray analysis targeted on library-derived transcripts revealed robust and reproducible enrichment, after selection, of cDNAs encoding the scaffolding adaptor Gab2. Gab2 was confirmed to strongly promote anchorage-independent growth when overexpressed. Interestingly, downregulation by RNAi of endogenous Gab2 in neoplastic cells did not affect their adherent growth, but abrogated their growth in soft agar. Gab2-driven anchorage independence was found to specifically involve activation of the Src-Stat3 signaling axis. A transcriptional "signature" of 205 genes was obtained from GAB2-transduced, anchorage-independent MCF10A cells, and found to contain two main functional modules, respectively controlling proliferation and cell adhesion/migration/invasion. Extensive validation on breast cancer datasets showed that the Gab2-signature provides a robust prognostic classifier for breast cancer metastatic relapse, largely independent from existing clinical and genomic indicators and from estrogen receptor status. This work highlights a pivotal role for GAB2 and its transcriptional targets in anchorage-independent growth and breast cancer metastatic progression.

Keywords: Gab2, anchorage independence, metastasis, microarray, breast cancer.

Introduction

Normal epithelial cells integrate signals from soluble ligands, like growth factors (GFs), cytokines and hormones, with signals derived from the binding of transmembrane integrins to the extracellular matrix (ECM), to ensure that they only proliferate in the 'correct' social context (Berrier and Yamada 2007). Joint integrin/GF signaling is required for cell proliferation and for optimal cell survival: cell adhesion enhances GF-dependent responses, like cell proliferation, migration and/or protection from apoptosis (Miranti and Brugge 2002). Conversely, cell detachment results in cellular desensitization to GF receptor signaling (Schwartz and Baron 1999). Moreover, signals evoked by integrins and GFs are widely integrated at the cellular level, since both impinge on an overlapping set of cytoplasmic signaling pathways (Berrier and Yamada 2007). Dependence on this reciprocal cross-talk is progressively lost by transformed cells during formation and spread of tumors (Guo and Giancotti 2004), and the acquisition of anchorage-independence is considered to be a crucial step during cancer progression towards invasion and metastasis (Tsatsanis and Spandidos 2004). Therefore, identification of genes or proteins promoting this step could provide novel targets or rationales for anti-cancer therapy. Among the possible ways for a genome-wide functional survey aimed at this scope are screenings based on the gain-of-function approach. Such screenings proved extremely valuable in the identification of genes involved in key cancer-related processes, like neoplastic transformation, resistance to apoptosis, or escape from senescence (Kitamura et al. 2003). As a screening model, we chose MCF10A cells, a spontaneously immortalized human breast line (Soule et al. 1990) that relies on both GFs and anchorage to proliferate. When these cells are cultured in the absence of anchorage, for instance on polyhema-coated plates, they undergo growth arrest and detachment-induced apoptosis, also known as anoikis (Reginato et al. 2003). It was previously shown that the low transforming potential of these cells renders them well-suited to monitor the effects of genes

conferring oncogenic properties (Debnath and Brugge 2005). Therefore, MCF10A cells represent an ideal model to screen for genes conferring anchorage-independence. For the screening we exploited a novel approach, named “Xenoarray analysis”, based on transduction of mammalian cells of a given species with an expression library from another species, followed by one-shot quantitative tracing with DNA microarrays of library-derived transcripts before and after a selective stress, to disclose genes conferring resistance to the selection (Martelli et al. 2008). After transduction with a mouse testis retroviral expression library, MCF10A cells were selected for growth in suspension and murine microarrays were used to compare signal intensities for the exogenous cDNAs before and after selection, to detect the enriched ones. Independent infection-selection experiments highlighted significant and reproducible enrichment for murine Gab2-encoding transcripts, suggesting a role of this gene in anchorage-independent growth. Through biochemical studies, cell-based assays and genomic analysis we found that Gab2 promotes anchorage-independent growth of normal and neoplastic cells, and drives a transcriptional program linked to metastatic progression of breast cancer.

Materials and methods

Cell Culture and Reagents.

MCF10A cells were obtained from ATCC and cultured as described (Reginato et al. 2003). MDA-MB-231 and MDA-MB-435 cells were obtained from ATCC and cultured in DMEM (Gibco) supplemented with 10% fetal bovine serum (Sigma). The antibodies used were: anti-Gab2 (Upstate Biotechnology), anti- Tyr416-phosphorylated Src (Cell Signaling), anti-total Src (Cell Signaling), anti-Tyr705-phosphorylated Stat3 (Cell Signaling), anti-total Stat3 (Cell Signaling), goat anti-actin (Santa Cruz). Retroviral expression library and pFB-hrGFP retroviral supernatant, packaged in the VSV envelope, were purchased from Stratagene (ViraPort, Cat n. 972300) and used to infect $1.5x10^5$ MCF10A cells in 60mm tissue culture plates using 10 µg/ml DEAE-dextran (Amersham Bioscence). GFP expression analysis was performed after 48 hours using a FACS Calibur flow cytometer (Becton Dickinson). Retroviral expression vector for GAB2 in pMIG (also known as pMSCV-IRES-GFP) was a gift of R. Daly. Virus production and transduction were performed as described (Brummer et al. 2006). Lentiviral shRNA expression vectors against murine or human GAB2 were purchased from Sigma (MISSION™ TRC shRNA Target Set), together with the pLKO.1-puro Control Vector. Viral supernatants were obtained according to the manufacturer's protocol. Infected cells were selected by puromycin treatment (2ug/ml for one week). Specific shRNA sequences which efficiently downregulated Gab2 protein, as assessed in Western blot, were the following: (i) Murine: CCGGCCGACACAATACAGAATTCAACTCGAGTTGAATTC-TGTATTGTGTCG-GTTTTTG; (ii) Human: CCGGCAGCCAACTCTGTTCACGTTTCTC-GAGAAACGTGAACAGAGTTGGCTGTTTTTTG.

Xenoarray and gene expression analysis

RNA was extracted using the Trizol Plus purification Kit (Invitrogen, cat.no.12183555), according to the manufacturer's protocol. Quantification and quality analysis of RNA was performed on a Bioanalyzer 2100 (Agilent). Synthesis of cDNA and biotinylated cRNA were performed using the Illumina TotalPrep RNA Amplification Kit (Ambion Cat. n. IL1791), according to the manufacturer's protocol, with previously reported variations in the case of Xenoarray analysis (Martelli et al. 2008), for which hybridization was carried out on Illumina Mouse6_V1 arrays. For standard microarray analysis of the Gab-2 signature, 1500 nanograms of cRNAs were hybridized on Illumina Beadarrays (Human_6_V2). All microarray data are available at GEO (*note: submission will be completed before publication*). To define genes associated with GAB2-driven anchorage independence, microarray data were normalized and filtered for expression and for not being differential between controls. Subsequently, statistical selection of differential genes was carried out as described in Supplementary Methods.

Anchorage-independent growth selection.

Polyhema-coated 10cm Petri dishes were prepared by applying 4ml of a 12mg/ml solution of poly-hydroxy-ethyl-methacrylate (polyhema; Sigma) in ethanol, *drying under tissue culture hood, repeating the application once and incubating the plates overnight at 37°C.* For the selection, 3 x 10^6 cells were plated onto polyhema-coated plates in complete growth medium. Cells were cultured in suspension for 48h then were let to recover on regular plates for 24h before repeating the selection cycle.

Western Blot.

Cell lysates from 2–5×10^6 cells were prepared in RIPA buffer (150 mM NaCl, 1% NP40, 0.5% DOC, 50 mM TrisHCL at pH 8, 0.1% SDS, 10% glycerol, 5 Mm EDTA, 20 mM NaF

and 1 mM Na3VO4) supplemented with 1 μg /ml each of pepstatin, leupeptin, aprotinin, and 200 μg/ml phenyl methylsulphonyl fluoride (PMSF). Lysates were cleared by centrifugation at 12,000 rpm for 20 min at 4°C and normalized with the BCA Protein Assay Reagent Kit (Pierce). Extracts were run on SDS-polyacrylamide gels, transferred onto nitrocellulose membranes (Hybond; GE Healthcare) and incubated with different antibodies overnight at 4°C. Nitrocellulose-bound antibodies were detected by the ECL system (GE Healthcare).

Real-time PCR.

Two micrograms of total RNA were reverse transcribed with the High Capacity cDNA Reverse Transcription Kit (Applied Biosystems, Foster City, CA). Quantitative Real-time PCR with Sybr Green was performed on the ABI Prism 7900HT Sequence Detection System (Applied Biosystems, Oak Brook, IL). *Details on PCR* primer design are available in Supplementary Methods.

Cell-based assays

For MTT cell growth assays, 10^3 cells were seeded in regular or polyhema-coated 96-well plates. Cells were cultured in growth medium containing all supplements or in starving medium (serum reduced to 2%, no EGF). At the indicated times, a tetrazolium salt–based reagent (CellTiter96 Aqueous One Solution, Promega) was added to each well according to the instructions provided by the manufacturer. After an incubation of 2 h, absorbance was read at 490 nm on a DTX 880 plate reader (Beckman Coulter). A control measurement after 4h from plating was used as a reference to adjust subsequent acquisitions of each cell line.

For soft agar growth, $3x10^4$ cells were resuspended in 2ml of 0.5% top agar (SeaPlaque Agarose from Cambrex) in growth medium and seeded in 6-well plates previously filled with 3ml of 1% basal agar in growth medium. The assay was performed in duplicate. After 3 weeks, phase-contrast pictures were captured by a BD Pathway microscopic station (BD

biosciences). Image analysis and quantification of single colonies number and size were performed by the Attovision 1.5 software (BD biosciences).

For detachment-induced cell death analysis, $3x10^5$ cells were plated on regular or polyhema-coated 35mm plates for 48 hours. Cell death was then measured by assessing the number of hypodiploid nuclei with the DNAcon3 kit (ConsulTS, Rivalta, Italy), according to the manufacturer's protocol and with cytofluorimetric analysis using a FACSCalibur (Becton Dickinson, San Diego, CA). Hypodiploid, subG0/G1 nuclei were defined as those displaying a PI staining value lower than that of cells in the G0/G1 cell cycle phase (diploid DNA peak).

Results

Setup of a gain-of-function screening for anchorage independence in MCF10A cells.

For the functional screening, MCF10A cells were transduced with a commercial mouse testis retroviral expression library (Stratagene) or with GFP as a control. To increase the screening robustness, infections were performed in duplicate (A and B), using an estimated multiplicity of infection of 1, to avoid multiple integrations in the same cell. To detect and quantify library-derived transcripts we performed Xenoarray analysis (Martelli et al. 2008), by extracting total RNA from the four cell populations and hybridizing the resulting cRNAs on murine expression arrays, to allow specific detection of library-derived transcripts of murine origin. Expression measurements obtained, for infections A and B, in GFP-transduced cells (x-axis) versus library-transduced cells were compared by scatter plot analysis (Supplementary Figure 1). Both library-transduced populations clearly showed a consistent number of detectable murine transcripts (945 and 1125 probes in infection A and B, respectively, with a detection p-value <0.01). Conversely, very few probes (around 100) cross-hybridized to endogenous transcripts and were detected also in GFP-transduced cells. Based on our previous observations on Xenoarray analysis sensitivity (Martelli et al. 2008), we estimated that a selection-driven 20-fold enrichment of even a rare transcript, bringing it from 8 to 160 parts per million, should be enough to render it clearly detectable by Xenoarray analysis.

We exploited the anchorage-dependence of MCF10A cells for a selective screening based on culturing GFP- or library-transduced cells on polyhema-coated plates. The four transduced populations were each split in two sub-lines: one was grown in adherence, the other underwent six cycles of selection, each cycle consisting of 48h of culture on polyhema

followed by 24h of recovery on regular plates. Cells recovered from GFP- and library-transduced cells after selection were named, respectively, “GFP-SEL” and “LIB-SEL”, and assayed for their ability to grow in the presence or absence of anchorage. LIB-SEL, but not GFP-SEL cells displayed significantly higher growth rate than unselected cells, in both adherence and suspension (Figure 1A). Moreover, as shown in Figure 1B-C, only LIB-SEL cells could form large colonies in soft agar, an *in vitro* hallmark of cell transformation. These findings confirmed a “library effect” not explainable with insertional mutagenesis but likely deriving from the expression of advantageous exogenous transcripts.

Identification by “Xenoarray” analysis of cDNAs conferring anchorage independence to MCF10A cells.

To identify library-derived transcripts promoting anchorage-independent growth, we conducted Xenoarray analysis on library-transduced cells, before and after selection (Supplementary Figure 2). A significant number of probes displayed higher signal in selected cells, indicating that cells expressing the respective transcripts were enriched by the selection. To identify the genes that were reproducibly enriched in both selections we calculated, for each transcript, the Log(2) ratio of the signal before and after selection. Interestingly, the Gab2 transcript showed a strong enrichment in both selections (average enrichment = 14-fold). The enrichment was observed with 3 different probes, each designed in a different region of the Gab2 transcript. Other genes, including Ntrk3 and Cyp11a1, displayed a stronger enrichment in selection A (respectively, 41- and 49-fold in selection A, and 2- and 1.3-fold in selection B). Quantitative Real-Time PCR analysis with mouse-specific primers confirmed that Gab2 was the most enriched transcript, followed by Cyp11a1 and Ntrk3 (Figure 2A). Therefore, we focused on this gene and validated its enrichment also at the protein level (Figure 2B), thereby showing that the exogenous cDNA enriched after the selection actually encodes the full-length Gab2 protein. Exogenous Gab2 was found to be

essential for anchorage-independent growth of the LIB-SEL population, as its downregulation by RNAi strongly reduced the growth advantage of LIB-SEL cells, in adhesion, in suspension and in soft agar (Supplementary Figure 3).

Validation and characterization of Gab2-driven anchorage-independence.

Gab2 is a scaffolding/docking protein involved in multiple signaling pathways downstream from membrane receptors (Nishida et al. 1999). To directly assess whether Gab2 may promote anchorage-independent growth, we transduced MCF10A cells with the human Gab2 coding sequence, cloned in a retroviral vector (gift of R. Daly;(Brummer et al. 2006)). The levels of exogenous Gab2 were comparable to those observed in the LIB-SEL population (Supplementary Figure 4). As shown in Figure 3A, adherent GAB2-overexpressing cells showed a significant increase in proliferation, which was further enhanced in the absence of anchorage. Notably, Gab2-driven growth advantage was almost totally lost when cells were kept in starving medium (no EGF, and serum lowered to 2%), indicating that Gab2 promotes proliferation independently from cell anchorage to the ECM, but dependently from the presence of GFs and/or serum. Accordingly, Gab2-overexpressing cells formed larger and more abundant colonies in soft agar, compared to wild-type cells (Figure 3B). Anchorage independence of Gab2-transduced MCF10A cells was again abrogated by Gab2 downregulation via RNAi (Supplementary Figure 5). To evaluate whether Gab2 promotes survival of detached cells, we estimated the fraction of dead cells after 48h of suspension culture. Surprisingly, after 48h of polyhema plating, we detected a comparable extent of cell death between wild-type and Gab2-expressing cells (Figure 3C). These data indicate that Gab2 is not involved in the protection of MCF10A cells from anoikis, but rather allows their proliferation in the absence of adhesion to the ECM.

Gab2-driven anchorage independence requires Src and involves Stat3.

Previous analyses have identified signaling molecules that can bind to Gab2 upon receptor activation, including the tyrosine phosphatase Ptpn11/Shp2, leading to activation of Erk and Jnk (Yu et al. 2006), the p85 subunit of PI3K, leading to Akt activation (Bouscary et al. 2001), and Src family kinases (Kong et al. 2003). Therefore, to dissect the signaling pathways downstream Gab2 that could mediate anchorage-independent growth, we examined the effects on cell vitality of a panel of small molecule inhibitors targeting the above mentioned signaling kinases (Figure 4A). The PI3K inhibitor was the most effective, but with no differential between anchorage-dependent and independent growth, or between control and Gab2-expressing cells, showing a general requirement of this pathway for survival of MCF10A cells. A similar but less pronounced effect was observed for Mek inhibition. The Jnk inhibitor displayed modest effects in all conditions. Interestingly, the Src inhibitor PP2 displayed the highest specificity towards Gab2-expressing cells in suspension. A more detailed analysis of the effects of Src inhibition is shown in Figure 4B. According to these data, Gab2-driven anchorage independence requires Src, which typically is activated by integrins when cells are adherent and becomes inactivated upon detachment (Playford and Schaller 2004). Consistently, western blot analysis on cell lysates from control and Gab2-expressing cells cultured in adhesion or suspension confirmed Gab2-driven activation of Src and of one of its downstream targets, Stat3 (Figure 4C). In adhesion, Gab2-expressing cells displayed a stronger basal phosphorylation of Src. Active Src levels were reduced in cells kept in suspension, but while in control cells Src activation was completely abolished at 48h, Gab2-expressing cells maintained some phosphorylation. Analysis of Stat3 activation highlighted an even more pronounced response to Gab2 expression, indicating the capacity of Gab2 to sustain the activation of Stat3 also in the absence of a substratum consensus. Since many studies provided evidence for Stat3 involvement in Src-mediated oncogenesis (Yu et al. 1995)

and anchorage-independent growth (Laird et al. 2003), these data indicate that Gab2 could signal through Src and Stat3 to accomplish anchorage-independent growth.

Endogenous Gab2 is essential for anchorage–independent growth of normal and neoplastic cells.

The data shown so far demonstrate that constitutive, exogenous expression of Gab2 promotes anchorage-independent growth. To verify if this effect is mirrored by physiologically controlled Gab2 expression, we silenced by RNAi the endogenous Gab2 in MCF10A and in human cancer cells (silencing efficacy is shown in Supplementary Figure 6). In MCF10A cells, Gab2 silencing markedly reduced their growth both in adhesion and in suspension (Figure 5A) while both MDA-MB-231 breast cancer cells and MDA-MB-435 melanoma cells responded to Gab2 silencing with a significant but modest reduction of proliferation (Figure 5B), indicating a minor role of Gab2 in the presence of attachment. Strikingly however, the ability of these cells to form colonies in soft agar was completely abrogated by Gab2 silencing (Figure 5C). In accordance with our previous western blot data, Gab2 loss determined a significant and concomitant decrease in Src and Stat3 activation (Figure 5D). Interestingly, the most evident reduction of Src-Stat3 phosphorylation was observed for MDA-MB 231 cells, which endogenously express the highest levels of Gab2 and most strongly reduce their soft agar growth upon Gab2 silencing. Altogether, these data confirmed the Gab2-Src-Stat3 axis as a key promoter of anchorage-independent growth of neoplastic cells.

A Gab2 transcriptional signature correlates with breast cancer aggressiveness.

To gain further insights on Gab2-driven anchorage-independence, we performed gene expression profiling on MCF10A cells transduced with Gab2 and selected by growth in the

absence of anchorage. As control, we used RNA extracted from GFP-transduced and selected cells. The selection was performed as described for the library-transduced cells. As further controls, GFP- and GAB2-transduced cells were profiled also before the selection, together with wild-type MCF10A cells (WT). Statistical analysis was applied to retrieve genes differentially expressed between GAB2-transduced and GFP-transduced cells after the selection (see Supplementary Methods), highlighting 221 probes, corresponding to 205 independent genes: the "GAB2-signature" (Supplementary Table 1). The signature revealed a significant enrichment ($p<2.5x10^{-5}$) in genes related to cell proliferation (also highlighted in Supplementary Table 1). Interestingly, the GAB2-signature was also significantly enriched in genes whose expression correlates to sensitivity of the NCI-60 panel of neoplastic cell lines to Resveratrol ($p=1x10^{-5}$), Piceatannol ($p=1x10^{-3}$) and SD-1029 ($p=1.2x10^{-4}$), small molecules that inhibit STAT3 activation by Src, Jak or other tyrosine kinases (see Supplementary Methods and Supplementary Table 2). These results confirm that the Src-STAT3 signaling axis plays a key role in GAB2-driven biological and transcriptional responses independently of tissue and cell type. To extend the value of the *in-vitro* model of Gab2-driven anchorage independence, we verified if the GAB2-signature could be associated to human breast cancer aggressiveness. To this aim, the signature was mapped on a 311-sample breast cancer dataset generated at the Netherland Cancer Institute on 2-color oligonucleotide microarrays (NKI dataset) and published in two works (van, V et al. 2002b; van, V et al. 2002a). After filtering for expression, the GAB2-signature was mapped to 150 probes. Interestingly, the signature resulted to be strongly enriched in genes discriminating breast cancer patients with or without metastatic recurrence within five years from the initial diagnosis ($p<10^{-8}$; see Supplementary Methods). On the basis of these results, using the nearest-mean classifier approach (Wessels et al. 2005), we built a classifier in the NKI dataset, based on the entire GAB2-signature, which provides a "Metastasis Score", MS, discriminating patients with good and poor

prognosis (Supplementary Methods and Supplementary Table 3). Data clustering and mining revealed two specific gene functional modules associated with prognosis: (i) a sizeable proliferation module positively correlated to metastatic progression, and (ii) an interesting module composed of negative regulators of cell-matrix interaction, migration and invasion, expressed at higher levels in good prognosis samples (Figure 6A and Supplementary Table 4). To validate the classifier, we mapped it on two independent datasets of 198 and 236 samples, both obtained on Affymetrix microarrays and aimed at evaluating, respectively, metastasis-free survival and death of disease (Desmedt et al. 2007; Miller et al. 2005). In both cases the Gab2-signature classified patients with high accuracy, despite the change of microarray platform (Figure 6B-C). We then applied the Gab2-signature on the 198-sample dataset stratified by various clinical and genomic classifiers originally provided in the work. When samples were subdivided by their prognostic class according to the Adjuvant!Online score (Hess 2008), they could still be further subdivided in good- and poor-prognosis subgroups by the GAB2-signature (Fig. 7A-B). Similarly, the GAB-2 signature correctly re-classified also samples previously subdivided in good- and poor-prognosis subgroups by genomic classifiers such as the 76-gene "Veridex Index" (Desmedt et al. 2007) (Fig. 7C-D) and the 70-gene "Mammaprint" classifier (Buyse et al. 2006) (Fig. 7E-F). These results show that the GAB2-signature predicts metastatic relapse of breast cancer independently of existing clinical and genomic classifiers. Such independence was further confirmed by univariate and multivariate statistics calculated, on the 198-sample dataset, for the Gab2 signature versus Adjuvant!online or three published genomic prognostic classifiers: Veridex index, MammaPrint and "Genomic Grade Index" (Sotiriou et al. 2006) (Table 1 and Supplementary Methods). Reciprocal significance impairment was only observed with the Mammaprint classifier, which, however, is obtained on a proprietary microarray platform, while the GAB2 signature can be directly tested on all publicly available Affymetrix microarray datasets. Finally, the GAB2-signature

was found to maintain prognostic ability also in samples subdivided by estrogen receptor (ER) status (Fig. 7G-H). Intriguingly, a small fraction of the ER-negative samples was called "good-prognosis" with 100% precision, but with no statistical significance probably due to the limited number (64) of samples analyzed. We therefore added samples from two other datasets (Ivshina et al. 2006; Wang et al. 2005), reaching a total of 175 ER-negative samples, for which the GAB2-signature maintained 100% precision and reached statistical significance (Supplementary Figure 7).

Discussion

To ensure successful metastatic dissemination, malignant cells must acquire the ability to grow in the absence of their environment of origin. In fact, the capacity of cells to survive and proliferate *in-vitro* in the absence of integrin-mediated adhesion strongly correlates with tumorigenesis *in-vivo* and may enable tumor cells to metastasize and grow at inappropriate sites in the body (Danen and Yamada 2001). We hereby describe a key role in anchorage-independent growth for Gab2, a multiadaptor protein devoid of enzymatic activity. The role of Gab2 in anchorage-independent growth emerged within the context of a high-throughput selective functional screening, in which this protein competed with several thousand others. Apart from GAB2, the analysis revealed a reproducible enrichment also for a well-known transforming gene, NTRK3, previously found to play a key role in anoikis resistance (Geiger and Peeper 2007) and useful as an internal control of the screening effectiveness. Gab2 is a member of the Grb2-associated binding protein (GAB) gene family (Gu et al. 1998). They are so called "scaffolding" or "docking" proteins because of the presence of multiple functional motifs mediating interactions with many other signaling molecules (Nishida et al. 1999). GAB proteins are involved in signaling events triggered by a variety of stimuli, including GFs, cytokines, G-coupled receptors and T- and B-lymphocyte antigens, ultimately regulating

cell growth, differentiation and transformation (Bouscary et al. 2001; Liu et al. 2001; Sattler et al. 2002). Among the Gab2 direct interactors are proteins with key roles in human cancer when mutated, such as PI3K and the tyrosine phosphatase Ptpn11/Shp2. Recent work suggested that the oncogenic properties of Ptpn11 mutant proteins require signal enhancement by Gab2 (Zatkova et al. 2006). Interestingly, Gab2 maps to a chromosomal region (11q13) amplified in 10-15% of breast cancers, and its overexpression was confirmed in several breast cancer cell lines (Daly et al. 2002). The role of Gab2 in mammary tumor metastasis was also explored and confirmed in mouse models (Ke et al. 2007). More recently, a key role for GAB2 in motility/invasion of melanoma cells and metastatic progression of melanoma was also highlighted (Horst et al. 2009). We now show that Gab2 also promotes anchorage-independent growth of breast cancer and melanoma cells. This information extends the previously described growth-promoting activity of Gab2 in adherent cells (Brummer et al. 2006). We also found that Gab2-driven anchorage independence is not due to a protection from cell death upon detachment. This finding was unexpected, given the fact that Gab2 potentiates the PI3k/Akt and Ras/Erk pathways, but it is in line with previous reports indicating that Gab2 does not prevent apoptosis of luminal cells during morphogenesis of MCF10A cells (tires-Alj et al. 2006). Our experiments using small molecule inhibitors showed that, while the PI3k/Akt and Ras/Erk pathways are required independently of the adhesion status and of Gab2 expression, Src inhibition had no effect on wild-type cells in suspension, but strongly impaired their adherent growth, confirming that Src conveys the proliferative consensus provided by integrin engagement (Playford and Schaller 2004). Moreover, Gab2-expressing cells required Src activity also in suspension, providing a strong rationale for Src involvement in Gab2-driven anchorage-independence. The biochemical link between Gab2 and Src can be provided by Ptpn11, previously described to directly bind Gab2 (Kong et al. 2003) and to activate Src (Zhang et al. 2004). It is of particular interest that Gab2-

sustained growth in suspension was impaired when cells were cultured in the absence of EGF, indicating that Gab2 can only overcome the lack of adhesive consensus in the presence of an upstream signal from GFs. Recently, Gab2 was found to promote GF independence in cooperation with oncogenic Src (Bennett et al. 2007). Therefore, Gab2 can rescue cells from the need of two concomitant proliferative stimuli - activated GF receptors and activated Src - when at least one of the two is present at sufficiently high levels. Therefore, Gab2 can be a key rheostat and integrator, allowing for a "spillover" of the signal across the two pathways, in the context of a network containing points of reciprocal influence and cross-talk (ffrench-Constant and Colognato 2004). In this view, proliferation of non-adherent cells could be promoted by a GF-driven direct activation of the Erk and Akt pathways and indirect, Gab2-mediated activation of Src and of its downstream signaling molecules, in particular Stat3. Indeed, Stat3 has been already involved in Src and Jak1-driven proliferation of human breast carcinoma cells (Garcia et al. 2001) and in anchorage-independent growth of cancer cells (Zhang et al. 2006). Moreover, Gab2 was found to contain a functional Stat3 binding motif promoting its recruitment and activation (Ni et al. 2007). Our biochemical data confirmed the contribution of Src and Stat3 to Gab2-mediated anchorage-independent growth: Gab2 expression increased Src and Stat3 phosphorylation both basally and after prolonged suspension culture, and Gab2 downregulation by RNAi led to reduction of Src and Stat3 activation not only in MCF10A cells constitutively expressing exogenous Gab2, but also in neoplastic cells loosing anchorage independence as a consequence of endogenous Gab2 silencing. In line with this, our gene expression analysis showed that a significant fraction of the genes whose expression is regulated by Gab2 are also differentially expressed in cancer cells resistant or sensitive to small molecule inhibitors of the Src/Jak1-STAT3 signaling axis. Finally, it is of particular significance that the Gab2 transcriptional signature yields a robust classifier for metastatic relapse of human breast cancer. Of the two key functional modules

found in the signature, the proliferation module, positively correlated with metastasis, adds further informative genes to the already described core of proliferation genes associated to breast cancer progression (Wirapati et al. 2008). More distinctive is the module of genes negatively correlated with metastasis, among which particularly interesting are: (i) two extracellular proteins that, respectively, inhibit matrix-degrading proteases (SERPINB1 (Cooley et al. 2001)) and remove fucose from ECM glycans (FUCA1), thereby impairing ECM binding and invasion by cancer cells (Yuan et al. 2008); (ii) the FAP gene, encoding an integral membrane protease whose expression is negatively correlated with metastatic progression (Ariga et al. 2001); (iii) PMP22, that encodes a 4-spanning integral membrane protein widely expressed at apical junctions of epithelial cells, increasing transepithelial electrical resistance and decreasing migration (Roux et al. 2005); (iv) the intracellular products of the ARHGDIB and SPRY1 genes, negative regulators of, respectively, Rho-family GTPases (DerMardirossian and Bokoch 2005) and tyrosine kinase receptors like EGFR and FGFR (Mason et al. 2006). These two functional modules, within the context of the GAB2-signature, generate a prognostic classifier predicting metastatic progression with high accuracy, independently from ER status and from other existing genomic signatures, and greatly outperforming the clinical-pathological prognostic parameters currently integrated into the Adjuvant!Online web tool (Hess 2008). Altogether, this work defines a key role for Gab2 in anchorage-independent growth of neoplastic cells and paves the way to prospective clinical validation of the GAB2-signature as a new, strong and independent prognostic classifier for breast cancer.

Acknowledgments

We thank Barbara Martinoglio and Roberta Porporato for technical assistance. We thank Simona Destefanis, Antonella Cignetto and Michela Bruno for secretarial assistance. This research was supported by grants from AIRC, the EC (contract n. 503438 “TRANSFOG”), CNR-MIUR, FIRB-MIUR, Ministero della Salute, Regione Piemonte and the Foundations CRT and ‘Compagnia di San Paolo’.

Conflict of interest.

E.M. is a member of the scientific advisory board of Proxenia and owns a patent on Xenoarray technology. C.I owns stocks in Proxenia. The remaining Authors declare no potential conflict of interest.

Supplementary Information

Supplementary information is available at Oncogene’s website.

References

Ariga N, Sato E, Ohuchi N, Nagura H and Ohtani H. (2001). Stromal expression of fibroblast activation protein/seprase, a cell membrane serine proteinase and gelatinase, is associated with longer survival in patients with invasive ductal carcinoma of breast. *Int J Cancer,* **95,** 67-72.

Bennett HL, Brummer T, Jeanes A, Yap AS and Daly RJ. (2007). Gab2 and Src co-operate in human mammary epithelial cells to promote growth factor independence and disruption of acinar morphogenesis. *Oncogene*.

Berrier AL and Yamada KM. (2007). Cell-matrix adhesion. *J Cell Physiol,* **213,** 565-573.

Bouscary D, Lecoq-Lafon C, Chretien S, Zompi S, Fichelson S, Muller O et al. (2001). Role of Gab proteins in phosphatidylinositol 3-kinase activation by thrombopoietin (Tpo). *Oncogene,* **20,** 2197-2204.

Brummer T, Schramek D, Hayes VM, Bennett HL, Caldon CE, Musgrove EA et al. (2006). Increased proliferation and altered growth factor dependence of human mammary epithelial cells overexpressing the Gab2 docking protein. *J Biol Chem,* **281,** 626-637.

Buyse M, Loi S, Van't VL, Viale G, Delorenzi M, Glas AM et al. (2006). Validation and clinical utility of a 70-gene prognostic signature for women with node-negative breast cancer. *J Natl Cancer Inst,* **98,** 1183-1192.

Cooley J, Takayama TK, Shapiro SD, Schechter NM and Remold-O'Donnell E. (2001). The serpin MNEI inhibits elastase-like and chymotrypsin-like serine proteases through efficient reactions at two active sites. *Biochemistry,* **40,** 15762-15770.

Daly RJ, Gu H, Parmar J, Malaney S, Lyons RJ, Kairouz R et al. (2002). The docking protein Gab2 is overexpressed and estrogen regulated in human breast cancer. *Oncogene,* **21,** 5175-5181.

Danen EH and Yamada KM. (2001). Fibronectin, integrins, and growth control. *J Cell Physiol,* **189,** 1-13.

Debnath J and Brugge JS. (2005). Modelling glandular epithelial cancers in three-dimensional cultures. *Nat Rev Cancer,* **5,** 675-688.

DerMardirossian C and Bokoch GM. (2005). GDIs: central regulatory molecules in Rho GTPase activation. *Trends Cell Biol,* **15,** 356-363.

Desmedt C, Piette F, Loi S, Wang Y, Lallemand F, Haibe-Kains B et al. (2007). Strong time dependence of the 76-gene prognostic signature for node-negative breast cancer patients in the TRANSBIG multicenter independent validation series. *Clin Cancer Res,* **13,** 3207-3214.

ffrench-Constant C and Colognato H. (2004). Integrins: versatile integrators of extracellular signals. *Trends Cell Biol,* **14,** 678-686.

Garcia R, Bowman TL, Niu G, Yu H, Minton S, Muro-Cacho CA et al. (2001). Constitutive activation of Stat3 by the Src and JAK tyrosine kinases participates in growth regulation of human breast carcinoma cells. *Oncogene,* **20,** 2499-2513.

Geiger TR and Peeper DS. (2007). Critical role for TrkB kinase function in anoikis suppression, tumorigenesis, and metastasis. *Cancer Res,* **67,** 6221-6229.

Gu H, Pratt JC, Burakoff SJ and Neel BG. (1998). Cloning of p97/Gab2, the major SHP2-binding protein in hematopoietic cells, reveals a novel pathway for cytokine-induced gene activation. *Mol Cell,* **2,** 729-740.

Guo W and Giancotti FG. (2004). Integrin signalling during tumour progression. *Nat Rev Mol Cell Biol,* **5,** 816-826.

Hess V. (2008). [Adjuvant!Online--an Internet-based decision tool for adjuvant chemotherapy in early breast cancer]. *Ther Umsch,* **65,** 201-205.

Horst B, Gruvberger-Saal SK, Hopkins BD, Bordone L, Yang Y, Chernoff KA et al. (2009). Gab2-mediated signaling promotes melanoma metastasis. *Am J Pathol,* **174,** 1524-1533.

Ivshina AV, George J, Senko O, Mow B, Putti TC, Smeds J et al. (2006). Genetic reclassification of histologic grade delineates new clinical subtypes of breast cancer. *Cancer Res,* **66,** 10292-10301.

Ke Y, Wu D, Princen F, Nguyen T, Pang Y, Lesperance J et al. (2007). Role of Gab2 in mammary tumorigenesis and metastasis. *Oncogene,* **26,** 4951-4960.

Kitamura T, Koshino Y, Shibata F, Oki T, Nakajima H, Nosaka T et al. (2003). Retrovirus-mediated gene transfer and expression cloning: powerful tools in functional genomics. *Exp Hematol,* **31,** 1007-1014.

Kong M, Mounier C, Dumas V and Posner BI. (2003). Epidermal growth factor-induced DNA synthesis. Key role for Src phosphorylation of the docking protein Gab2. *J Biol Chem,* **278,** 5837-5844.

Laird AD, Li G, Moss KG, Blake RA, Broome MA, Cherrington JM et al. (2003). Src family kinase activity is required for signal tranducer and activator of transcription 3 and focal adhesion kinase phosphorylation and vascular endothelial growth factor signaling in vivo and for anchorage-dependent and -independent growth of human tumor cells. *Mol Cancer Ther,* **2,** 461-469.

Liu Y, Jenkins B, Shin JL and Rohrschneider LR. (2001). Scaffolding protein Gab2 mediates differentiation signaling downstream of Fms receptor tyrosine kinase. *Mol Cell Biol,* **21,** 3047-3056.

Martelli ML, Isella C, Mira A, Fu L, Cantarella D and Medico E. (2008). Exploiting orthologue diversity for systematic detection of gain-of-function phenotypes. *BMC Genomics,* **9,** 254.

Mason JM, Morrison DJ, Basson MA and Licht JD. (2006). Sprouty proteins: multifaceted negative-feedback regulators of receptor tyrosine kinase signaling. *Trends Cell Biol,* **16,** 45-54.

Miller LD, Smeds J, George J, Vega VB, Vergara L, Ploner A et al. (2005). An expression signature for p53 status in human breast cancer predicts mutation status, transcriptional effects, and patient survival. *Proc Natl Acad Sci U S A,* **102,** 13550-13555.

Miranti CK and Brugge JS. (2002). Sensing the environment: a historical perspective on integrin signal transduction. *Nat Cell Biol,* **4,** E83-E90.

Ni S, Zhao C, Feng GS, Paulson RF and Correll PH. (2007). A novel Stat3 binding motif in Gab2 mediates transformation of primary hematopoietic cells by the Stk/Ron receptor tyrosine kinase in response to Friend virus infection. *Mol Cell Biol,* **27,** 3708-3715.

Nishida K, Yoshida Y, Itoh M, Fukada T, Ohtani T, Shirogane T et al. (1999). Gab-family adapter proteins act downstream of cytokine and growth factor receptors and T- and B-cell antigen receptors. *Blood,* **93,** 1809-1816.

Playford MP and Schaller MD. (2004). The interplay between Src and integrins in normal and tumor biology. *Oncogene,* **23,** 7928-7946.

Reginato MJ, Mills KR, Paulus JK, Lynch DK, Sgroi DC, Debnath J et al. (2003). Integrins and EGFR coordinately regulate the pro-apoptotic protein Bim to prevent anoikis. *Nat Cell Biol,* **5,** 733-740.

Roux KJ, Amici SA, Fletcher BS and Notterpek L. (2005). Modulation of epithelial morphology, monolayer permeability, and cell migration by growth arrest specific 3/peripheral myelin protein 22. *Mol Biol Cell,* **16,** 1142-1151.

Sattler M, Mohi MG, Pride YB, Quinnan LR, Malouf NA, Podar K et al. (2002). Critical role for Gab2 in transformation by BCR/ABL. *Cancer Cell,* **1,** 479-492.

Schwartz MA and Baron V. (1999). Interactions between mitogenic stimuli, or, a thousand and one connections. *Curr Opin Cell Biol,* **11,** 197-202.

Sotiriou C, Wirapati P, Loi S, Harris A, Fox S, Smeds J et al. (2006). Gene expression profiling in breast cancer: understanding the molecular basis of histologic grade to improve prognosis. *J Natl Cancer Inst,* **98,** 262-272.

Soule HD, Maloney TM, Wolman SR, Peterson WD, Jr., Brenz R, McGrath CM et al. (1990). Isolation and characterization of a spontaneously immortalized human breast epithelial cell line, MCF-10. *Cancer Res,* **50,** 6075-6086.

tires-Alj M, Gil SG, Chan R, Wang ZC, Wang Y, Imanaka N et al. (2006). A role for the scaffolding adapter GAB2 in breast cancer. *Nat Med,* **12,** 114-121.

Tsatsanis C and Spandidos DA. (2004). Oncogenic kinase signaling in human neoplasms. *Ann N Y Acad Sci,* **1028,** 168-175.

van ', V, Dai H, van d, V, He YD, Hart AA, Mao M et al. (2002a). Gene expression profiling predicts clinical outcome of breast cancer. *Nature,* **415,** 530-536.

van d, V, He YD, van't Veer LJ, Dai H, Hart AA, Voskuil DW et al. (2002b). A gene-expression signature as a predictor of survival in breast cancer. *N Engl J Med,* **347,** 1999-2009.

Wang Y, Klijn JG, Zhang Y, Sieuwerts AM, Look MP, Yang F et al. (2005). Gene-expression profiles to predict distant metastasis of lymph-node-negative primary breast cancer. *Lancet,* **365,** 671-679.

Wessels LF, Reinders MJ, Hart AA, Veenman CJ, Dai H, He YD et al. (2005). A protocol for building and evaluating predictors of disease state based on microarray data. *Bioinformatics,* **21,** 3755-3762.

Wirapati P, Sotiriou C, Kunkel S, Farmer P, Pradervand S, Haibe-Kains B et al. (2008). Meta-analysis of gene expression profiles in breast cancer: toward a unified understanding of breast cancer subtyping and prognosis signatures. *Breast Cancer Res,* **10,** R65.

Yu CL, Meyer DJ, Campbell GS, Larner AC, Carter-Su C, Schwartz J et al. (1995). Enhanced DNA-binding activity of a Stat3-related protein in cells transformed by the Src oncoprotein. *Science,* **269,** 81-83.

Yu M, Luo J, Yang W, Wang Y, Mizuki M, Kanakura Y et al. (2006). The scaffolding adapter Gab2, via Shp-2, regulates kit-evoked mast cell proliferation by activating the Rac/JNK pathway. *J Biol Chem,* **281,** 28615-28626.

Yuan K, Listinsky CM, Singh RK, Listinsky JJ and Siegal GP. (2008). Cell surface associated alpha-L: -fucose moieties modulate human breast cancer neoplastic progression. *Pathol Oncol Res,* **14,** 145-156.

Zatkova A, Schoch C, Speleman F, Poppe B, Mannhalter C, Fonatsch C et al. (2006). GAB2 is a novel target of 11q amplification in AML/MDS. *Genes Chromosomes Cancer*, **45,** 798-807.

Zhang SQ, Yang W, Kontaridis MI, Bivona TG, Wen G, Araki T et al. (2004). Shp2 regulates SRC family kinase activity and Ras/Erk activation by controlling Csk recruitment. *Mol Cell,* **13,** 341-355.

Zhang W, Zong CS, Hermanto U, Lopez-Bergami P, Ronai Z and Wang LH. (2006). RACK1 recruits STAT3 specifically to insulin and insulin-like growth factor 1 receptors for activation, which is important for regulating anchorage-independent growth. *Mol Cell Biol,* **26,** 413-424.

Figure Legends

Figure 1. Xenoarray analysis on MCF10A cells and acquisition of anchorage independence by library-transduced selected cells. (A) MTT growth assay on polyhema-selected populations after 48h and 72h in adhesion or suspension, as indicated. Cell growth is expressed as a ratio between library-transduced and GFP-transduced cells, after normalization to the amount of viable plated cells at day 0. The data represent the mean and standard error of triplicate values (Adhesion 48h $p<0.05$, Suspension 48h $p<0.01$, Suspension 72h $p<0.05$). (B) Soft agar assay on GFP- and library-transduced cells, unselected or selected on polyhema, as indicated. Phase-contrast images were captured by a BD Pathway microscopic station (BD biosciences) after 3 weeks in agar. (C) Dot plot of single colony sizes as calculated by the Attovision software (BD Biosciences, version 1.5) for the GFP-SEL and LIB-SEL populations grown in soft agar.

Figure 2. Identification of enriched cDNAs in anchorage-independent, library-transduced MCF10A cells. (A) Real-time PCR validation of enriched transcripts in both selections. The y-axis represents the relative increase in abundance of the transcripts in selected cells compared to unselected cells. (B) Western blot analysis on GFP- and library-transduced cells before and after selection to detect Gab2 protein enrichment.

Figure 3. Gab2 overexpression promotes anchorage-independent growth of MCF10A cells. (A) Box-plot of an MTT growth assay on Mock- (M) or Gab2- (G) transduced MCF10A cells in adhesion or suspension, in the presence of complete medium or of starving medium (no EGF and 2% serum) for 48 hours. Cell vitality was normalized to the amount of cells in Mock-transduced, adherent cells in complete medium after 48 hours (CTRL) The data were

obtained in triplicates, and t-test highlighted significant differences between G and M cells only in complete medium (* = $p<0.01$, ** = $p<0.0001$) (B) Dot plot of single colony sizes as calculated by the Attovision software (BD Biosciences, version 1.5) for the Mock and GAB2 cell populations grown in soft agar. (C) Flow cytometry analysis of apoptosis induction for Mock and Gab2-expressing MCF10A. Cell death was measured after 48h either in adhesion or suspension, by assessing the number of hypodiploid nuclei with the DNAcon3 kit. The percent of apoptotic cells is reported on the y-axis.

Figure 4. Evaluation of the contribution of different signaling pathways to Gab2-mediated enhancement of cell growth. (A) Mock and GAB2-overexpressing (GAB2) MCF10A cells were incubated in adhesion (ADH) or suspension (SUSP) in the presence or absence of MEK inhibitor (PD98059, 40μM), PI3K inhibitor (LY294002, 50μM), Src inhibitor (PP2, 10μM), or JNK inhibitor (SP600125, 10μM). Cell vitality was assessed with the MTT assay after 24h from the treatment and the drug effect was expressed as percent growth inhibition (with respect to untreated cells). The data represent the mean and standard error of triplicate values from two independent experiments. (B) Boxplots of detailed analysis of the effects of Src inhibition by PP2 on cell growth in various conditions. Cell growth, measured by the MTT assay, is expressed as percent of untreated Mock, adherent cells. The data were obtained in triplicates, and t-test highlighted significant responses to PP2 in all cases except for mock cells in suspension (* = $p<0.05$, ** = $p<0.005$). (C) Western blot analysis on Mock and Gab2-expressing cells in adhesion or after 24h and 48h in suspension. Antibodies directed against the activated form of Src (phosphorylated at tyrosine 416) and Stat3 (phosphorylated at tyrosine 705), or total Src or Stat3 were used.

Figure 5. Knock-down of endogenous Gab2 impairs MCF10A growth and anchorage-independent growth of human neoplastic cells. (A) MTT growth assay on wild-type MCF10A cells transduced with a scramble vector (CTRL) or a Gab2-shRNA in adhesion or suspension for 48h. Cell vitality was normalized to the amount of viable plated cells at time 0 and visualized independently for both cells by boxplots. The data were obtained in quintuplicate using two different GAB2-targeting shRNAs, and t-test highlighted significant differences between CTRL and GAB2-shRNA cells both in adhesion and suspension (* = $p<5x10^{-3}$, ** = $p<5x10^{-8}$). (B) MTT growth assay on MDA-MB-231 and MDA-MB-435 cells transduced with scramble vector (CTRL) or Gab2-shRNA in adhesion or suspension for 48h. Cell vitality was normalized to the amount of viable plated cells at time 0 and visualized independently for both cells by boxplots. The data were obtained in sextuplicate, and t-test highlighted modestly significant differences between CTRL and GAB2-shRNA cells in both MDA-MB-231 and MDA-MB-435 cells (* = $p<0.05$). (C) Soft agar growth of cells expressing Gab2 shRNA or scramble vector (CTRL). Phase-contrast images were captured by a BD Pathway microscopic station (BD biosciences) after 3 weeks in agar. (D) Western blot analysis of Src and Stat3 activation in control and GAB2 shRNA-transduced cells, as indicated.

Figure 6. The GAB2-signature predicts breast cancer metastatic relapse. (A) Heatmap showing the expression of the two main gene functional modules in the NKI-311 breast cancer dataset. The samples (columns) are ordered by decreasing GAB2-signature metastasis score (GAB2 MTS Score), which is graphically reported in the second row. The first row shows the occurrence of metastatic relapse within five year. The arrow at the bottom indicates the -0.15 threshold of metastasis score discriminating good and poor prognosis samples, also highlighted by a white vertical line crossing the heatmap. Green and red dots on the right

highlight the genes annotated to the two functional modules, respectively downregulated and upregulated in poor prognosis samples. (B) Kaplan-Meier analysis of metastasis-free survival on a dataset of 198 breast cancer samples classified as good prognosis (green line) or poor prognosis (red line) by the GAB2-signature. (C) Kaplan-Meier analysis of disease-specific survival on a dataset of 236 breast cancer samples classified as good prognosis (green line) or poor prognosis (red line) by the GAB2-signature.

Figure 7. The GAB2-signature is independent from existing clinical and genomic breast cancer classifiers, and from estrogen receptor status. (A-F) Kaplan-Meier analysis on the 198-samples dataset subdivided in two prognostic subgroups (A,C,E = poor prognosis, B,D,F = good prognosis) by the Adjyvant!Online clinical score (A-B), the Veridex Index (C-D) and the Mammaprint classifier (E-F). Each subgroup is then further subdivided by the GAB2-signature in good prognosis (green line) or poor prognosis (red line) samples. (G-H) Kaplan-Meier analysis on the 198-samples dataset subdivided in ER-negative (G) and ER-positive (H) samples, then further subdivided by the GAB2-signature in good prognosis (green line) or poor prognosis (red line) samples.

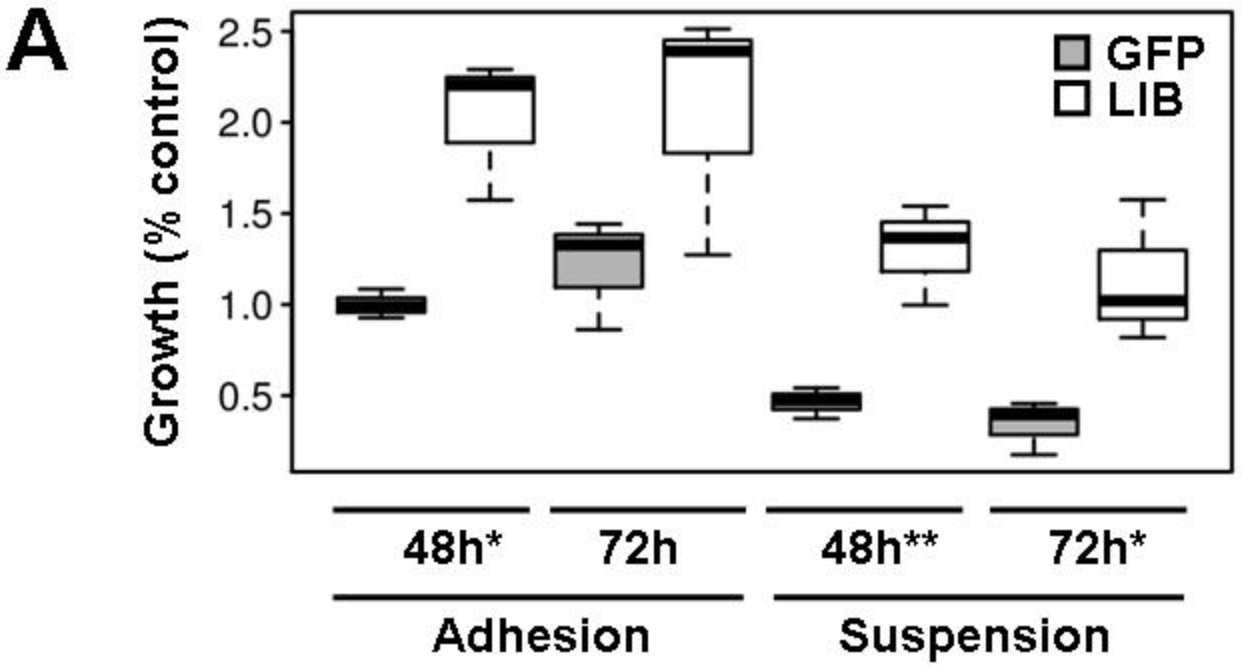

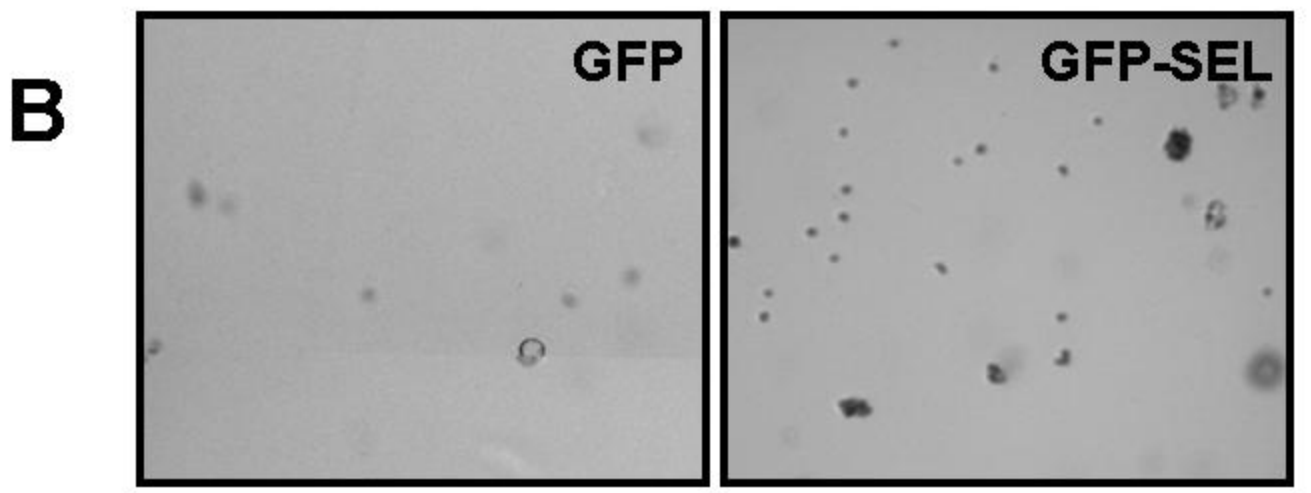

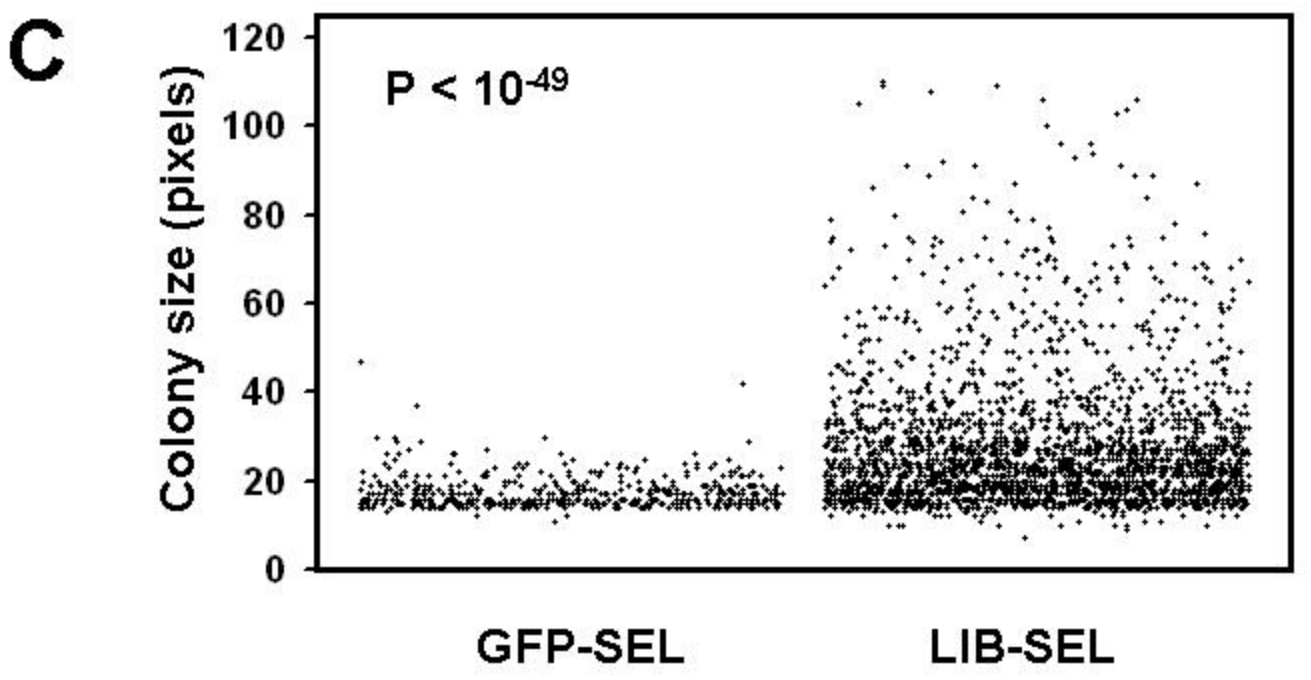

Mira et al., Figure 1

A

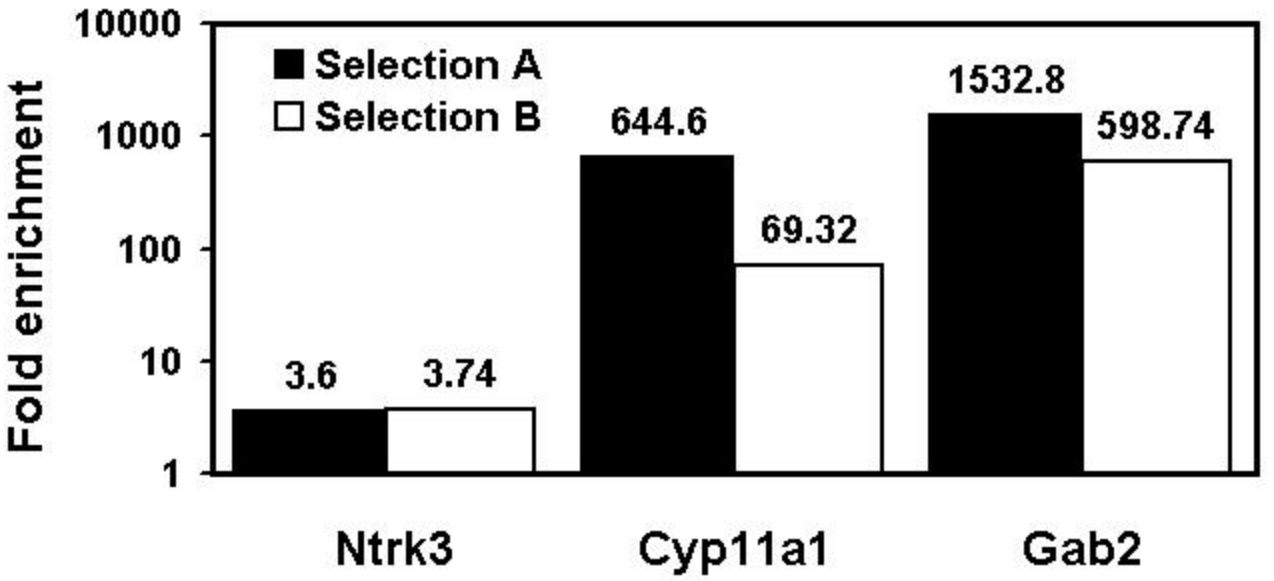

B

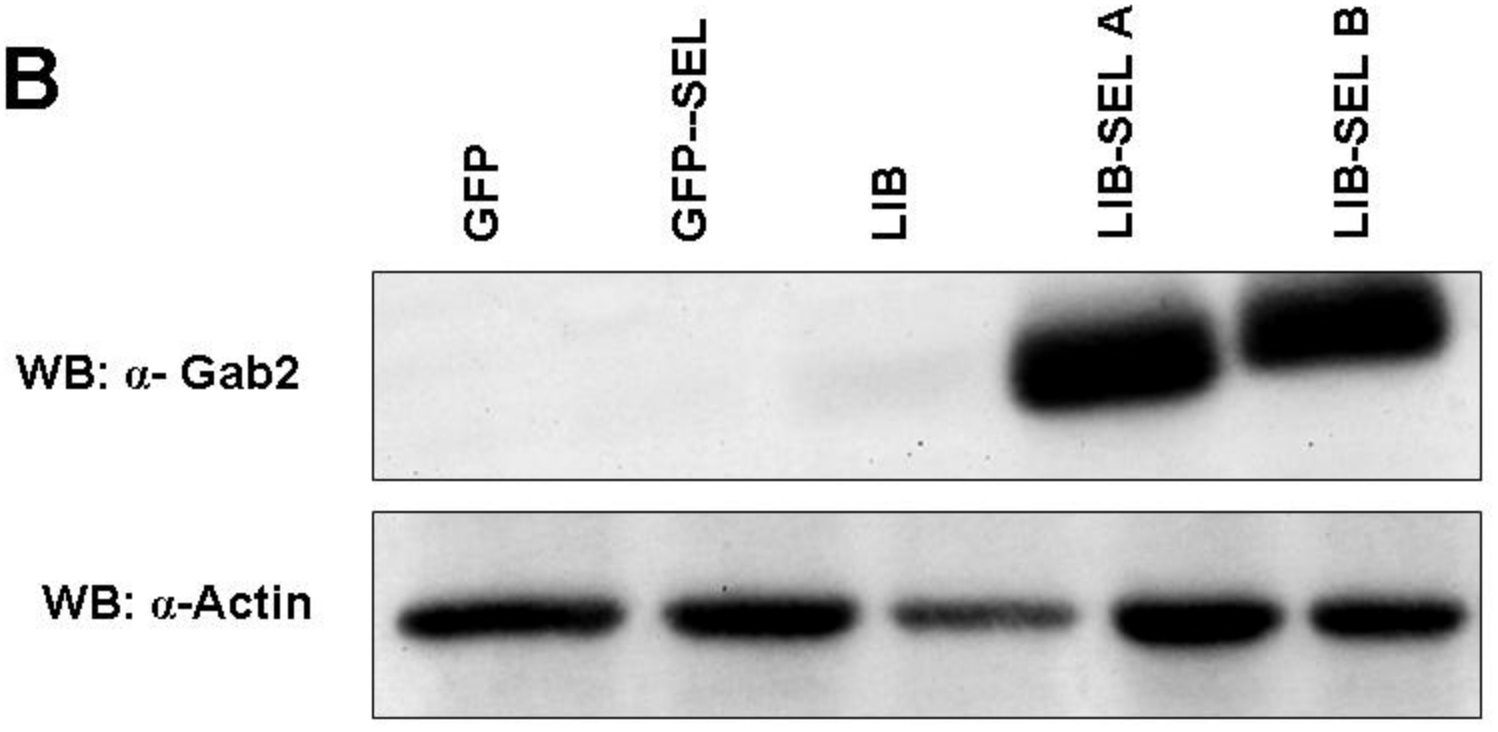

Mira et al., Figure 2

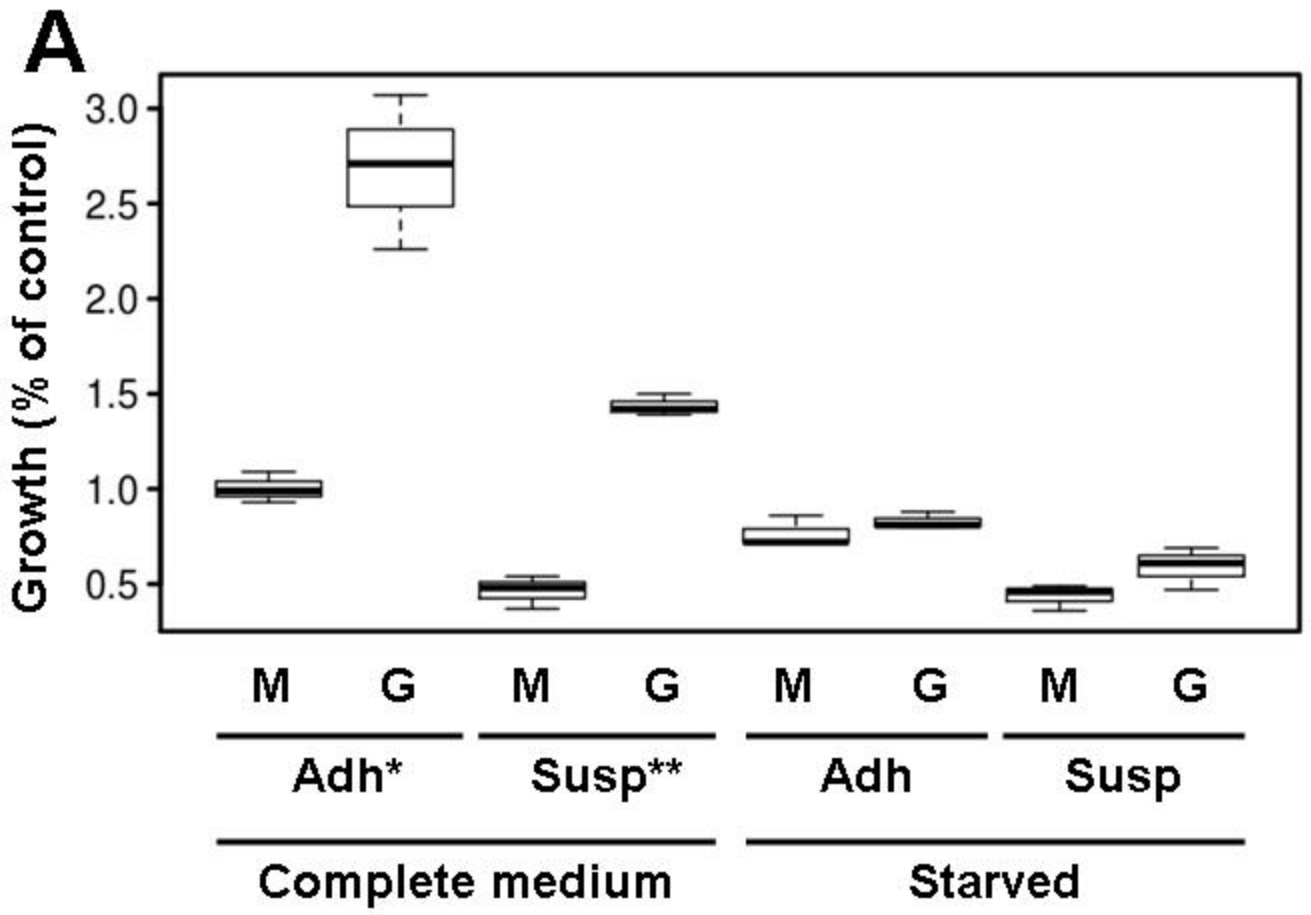

Mira et al., Figure 3

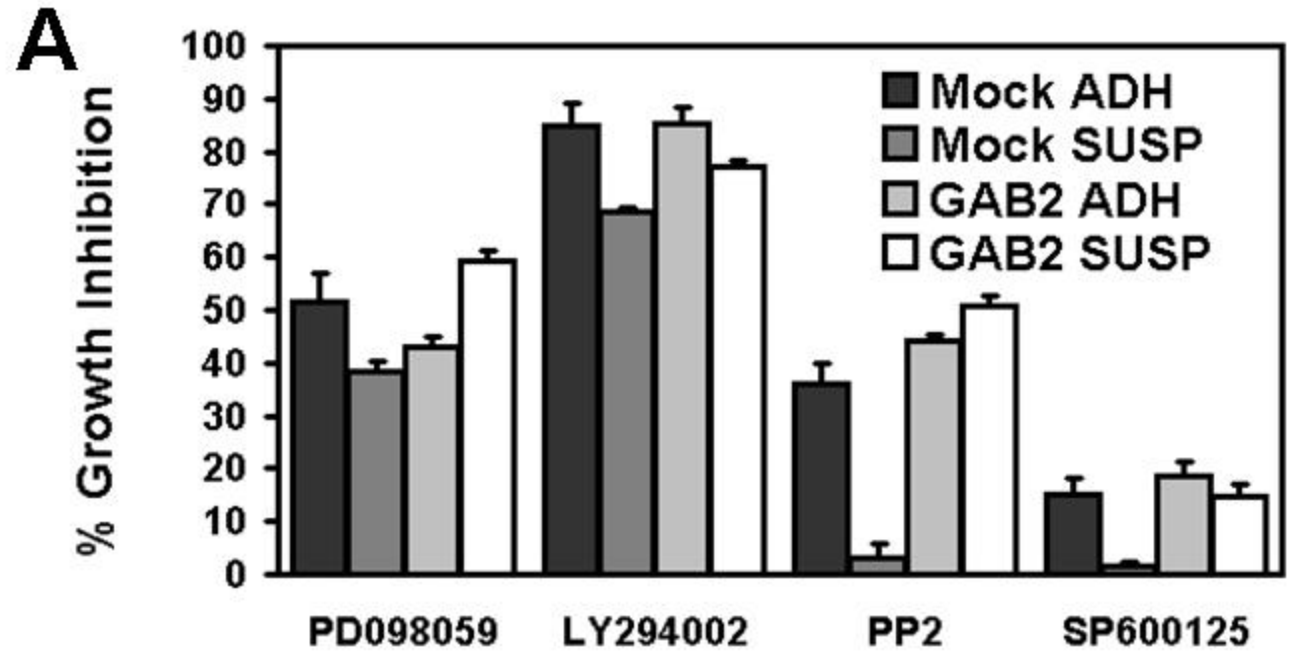

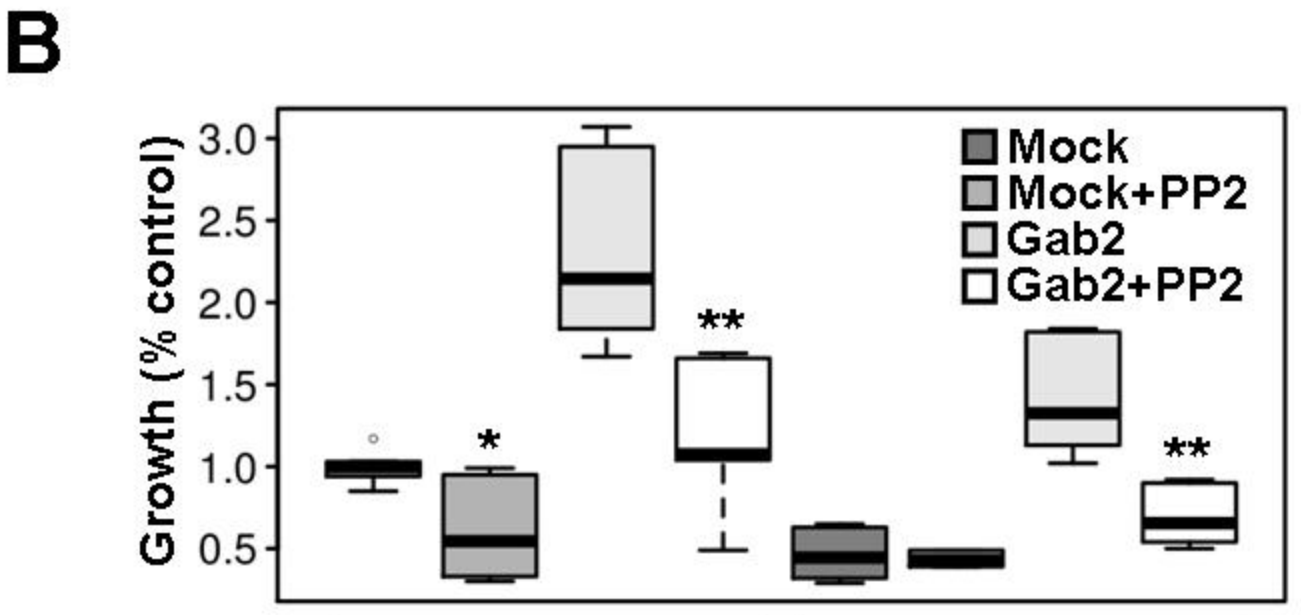

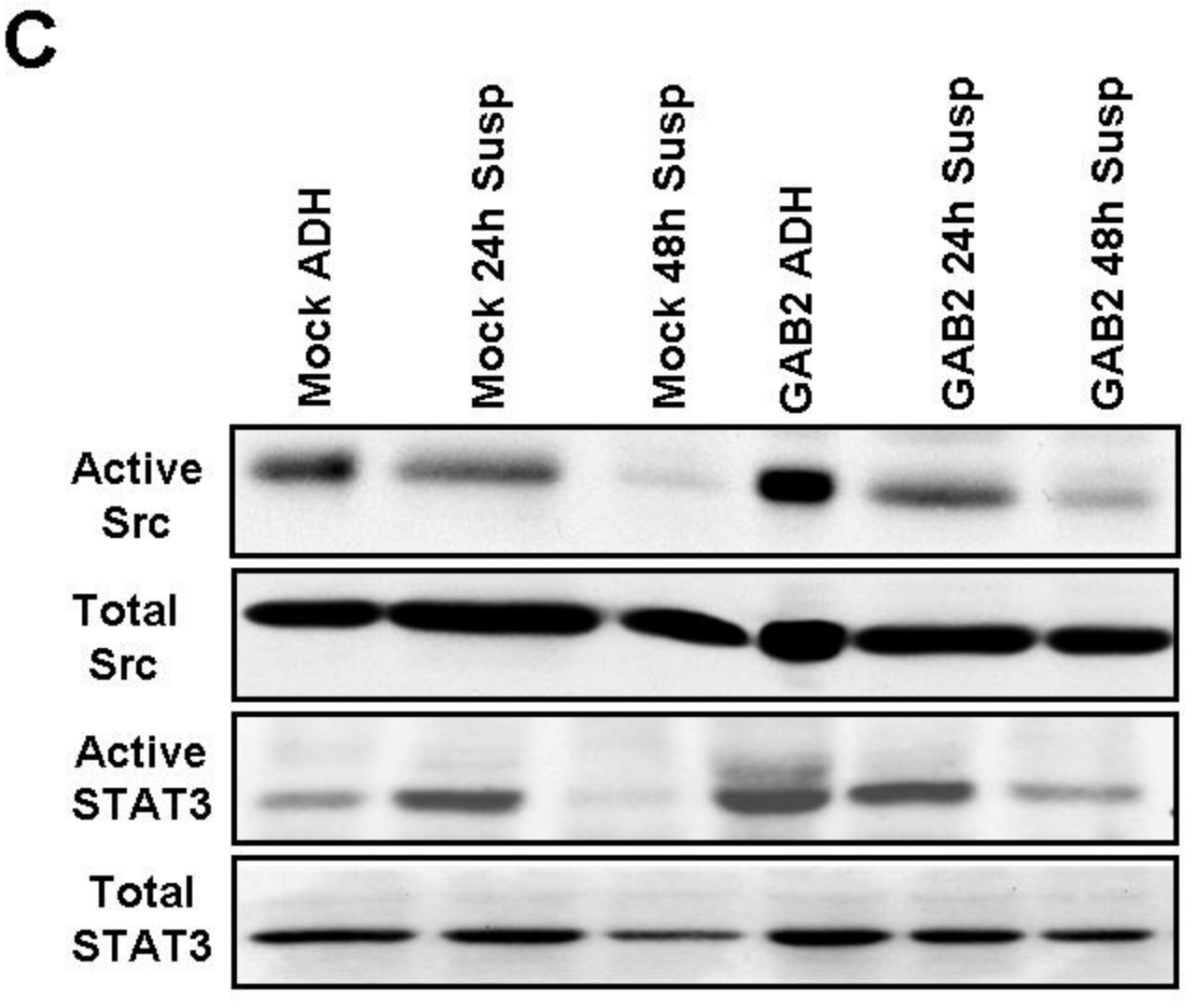

Mira et al., Figure 4

A

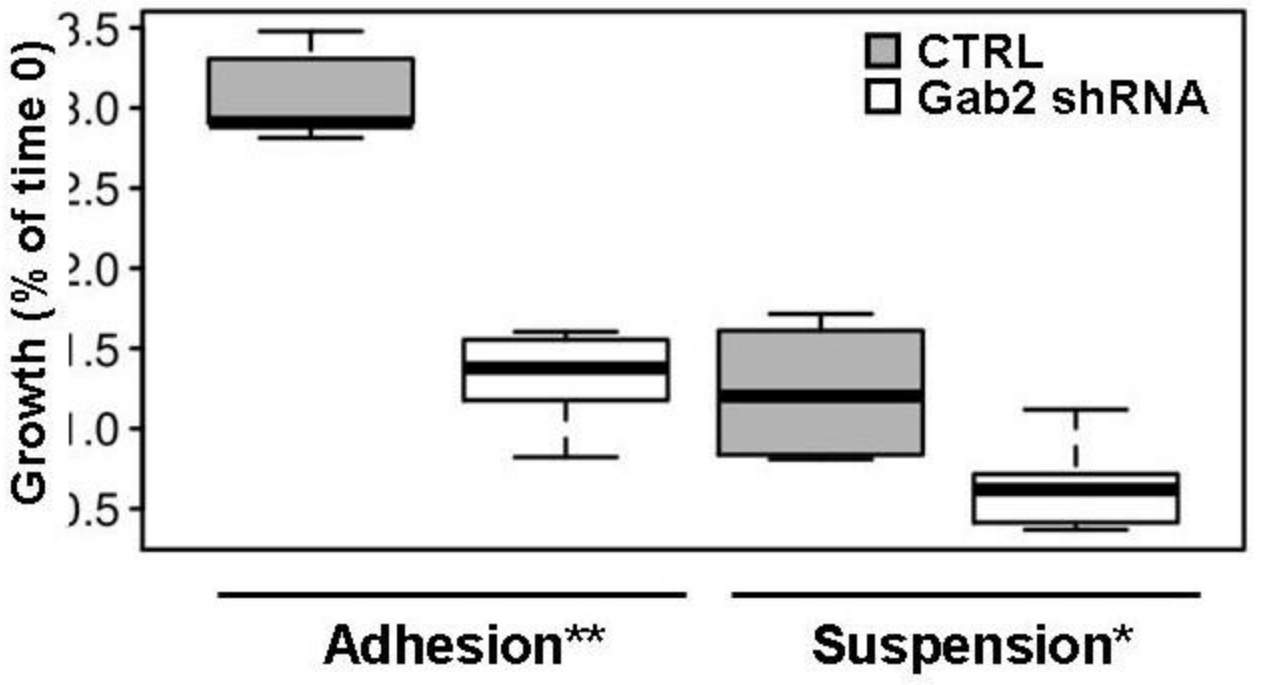

B

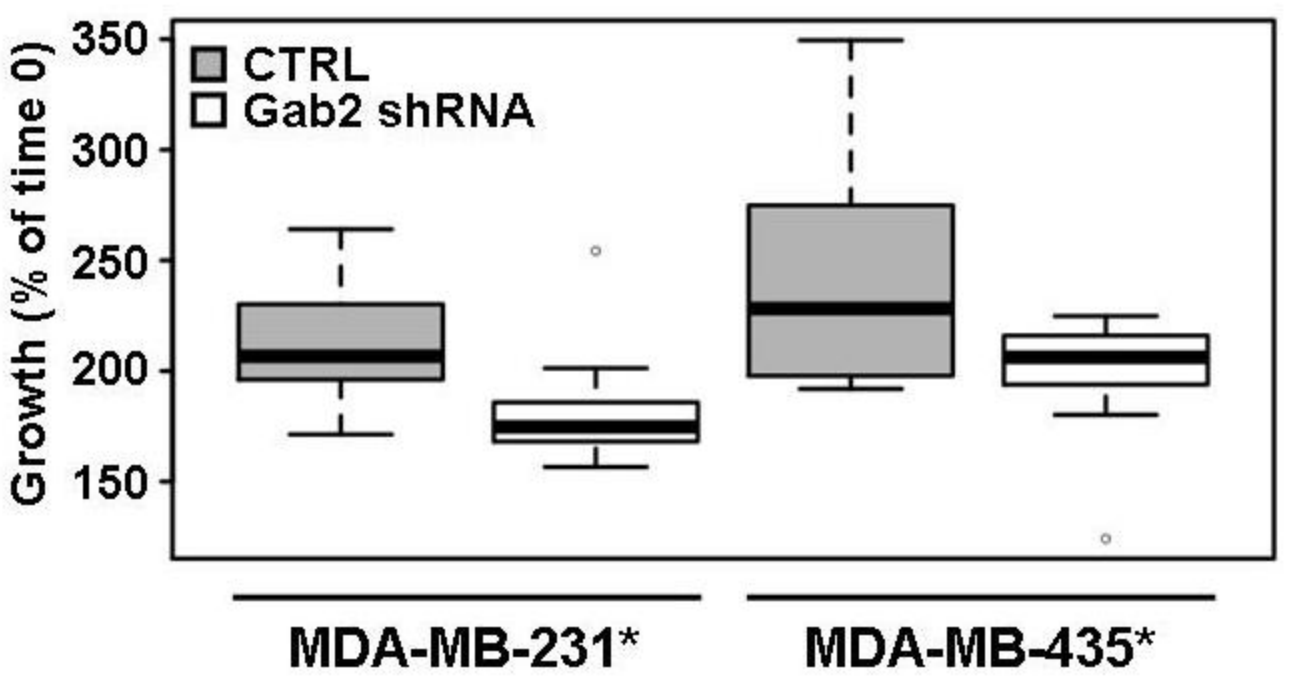

C

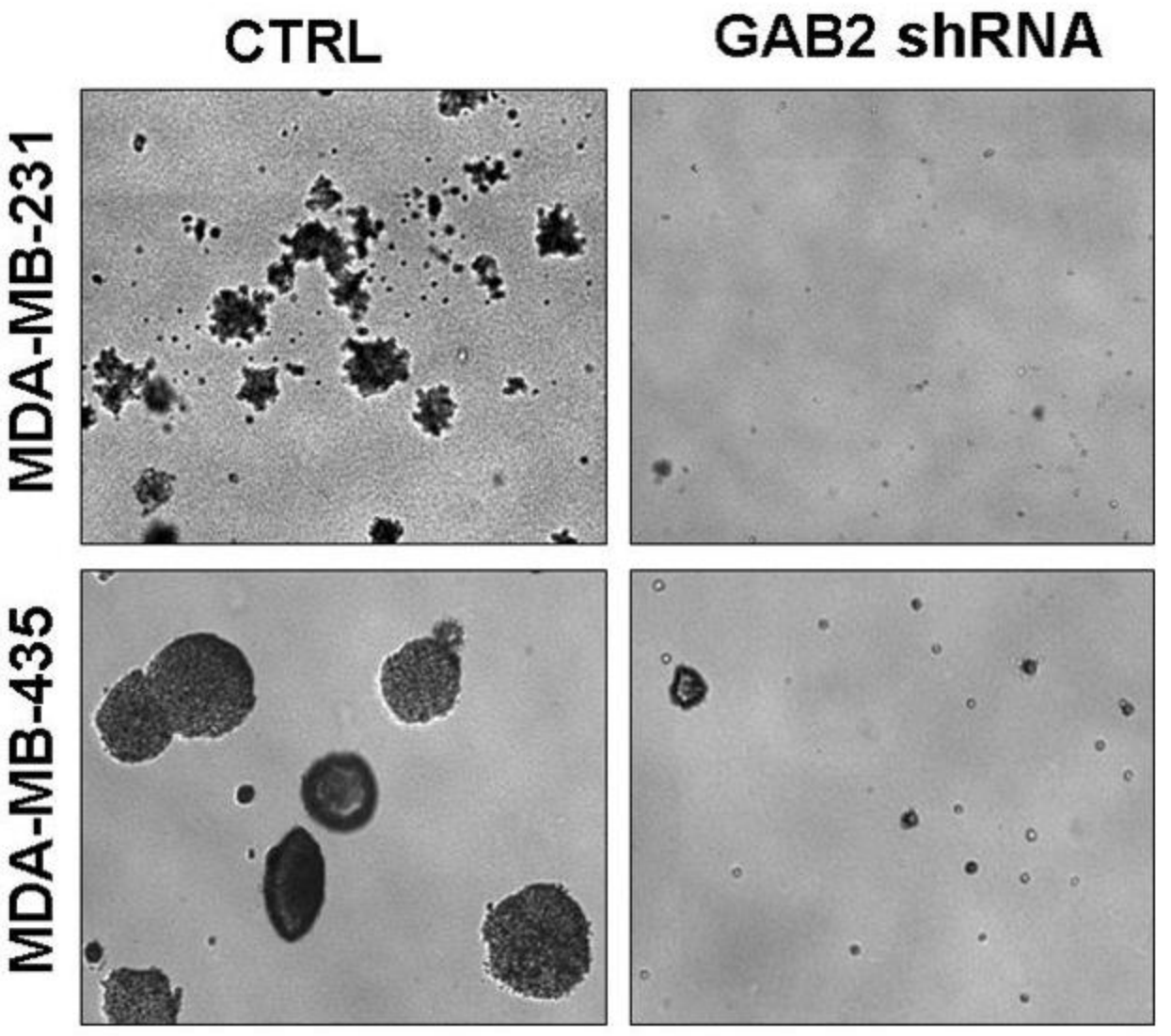

D

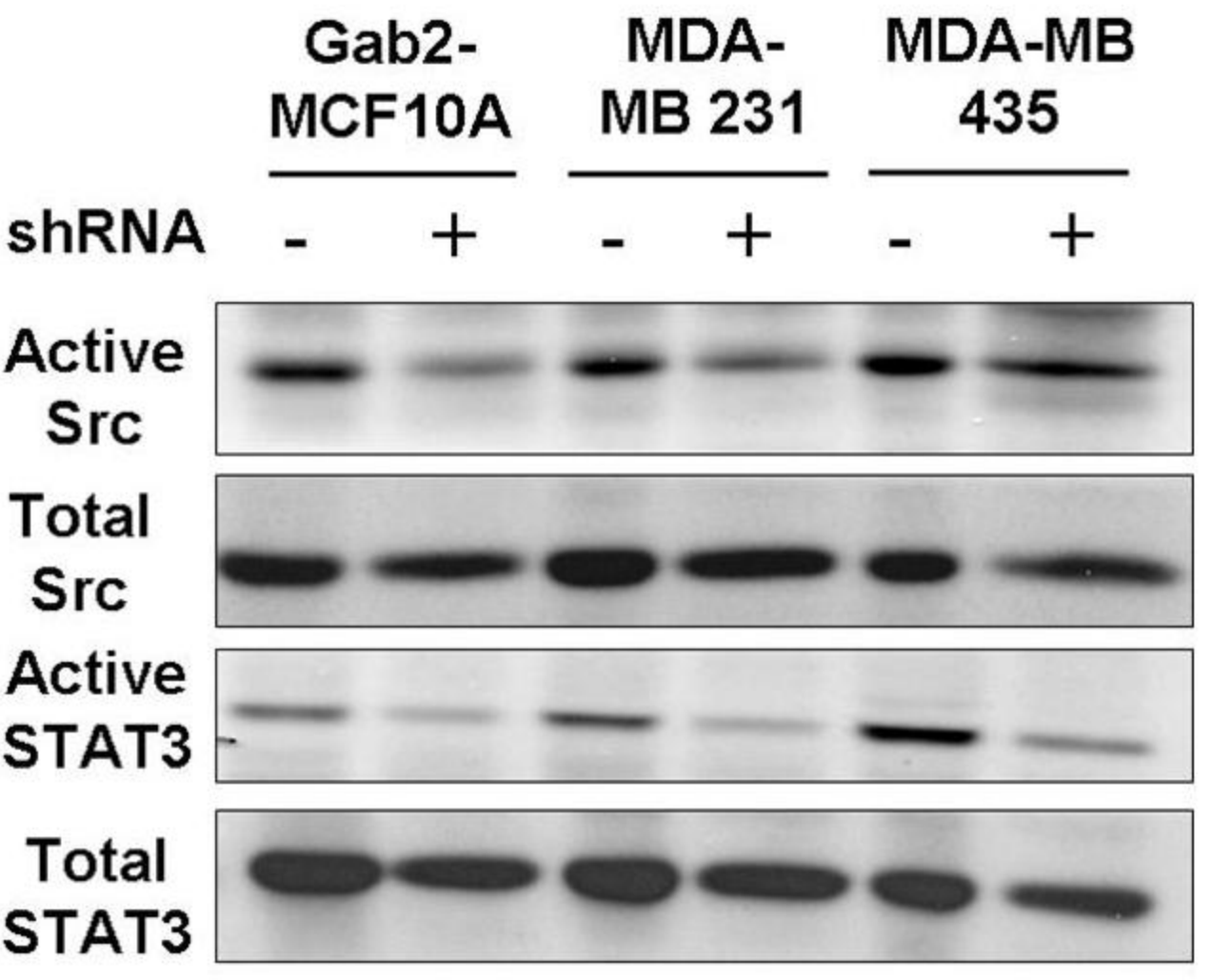

Mira et al., Figure 5

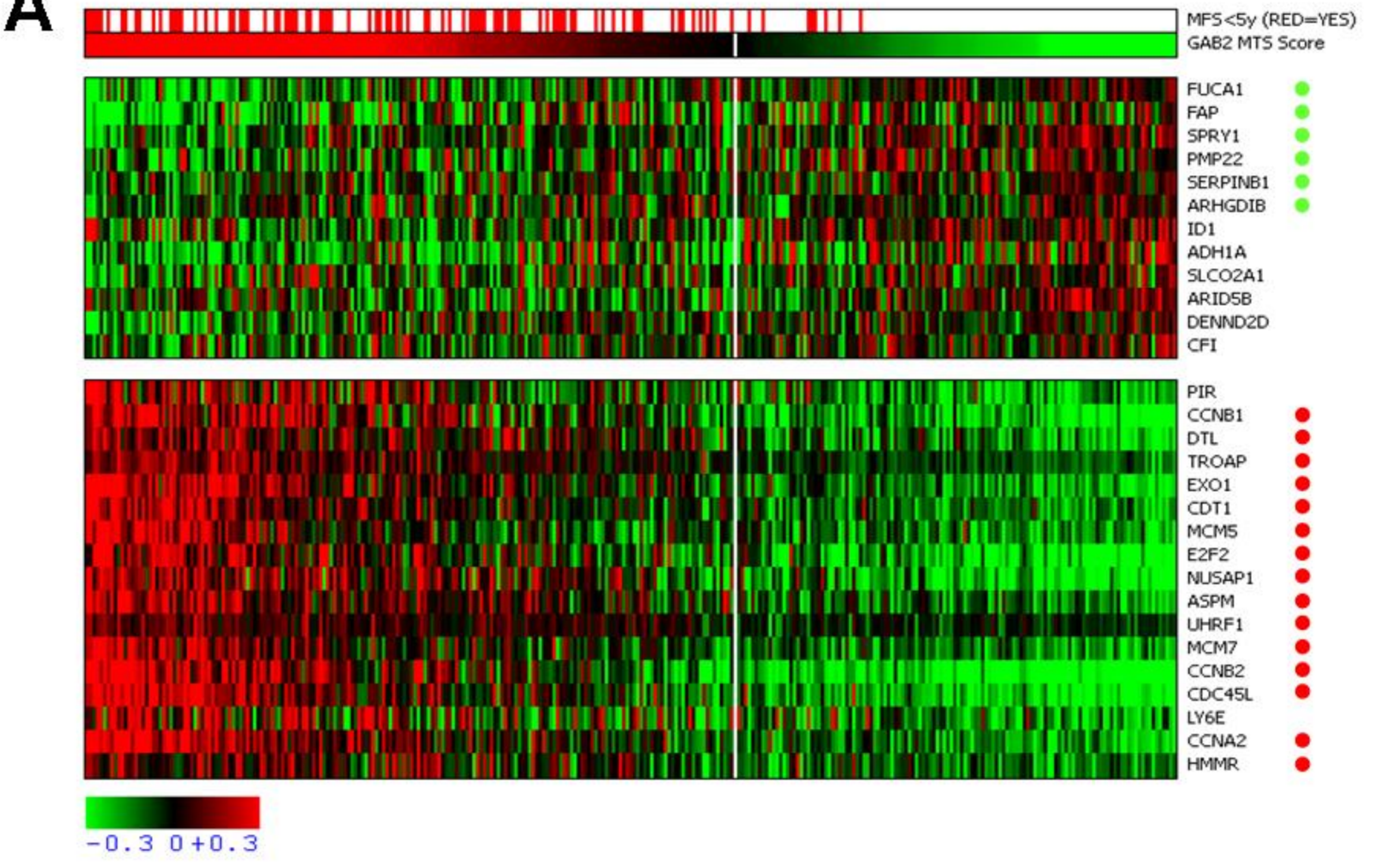

Mira et al., Figure 6

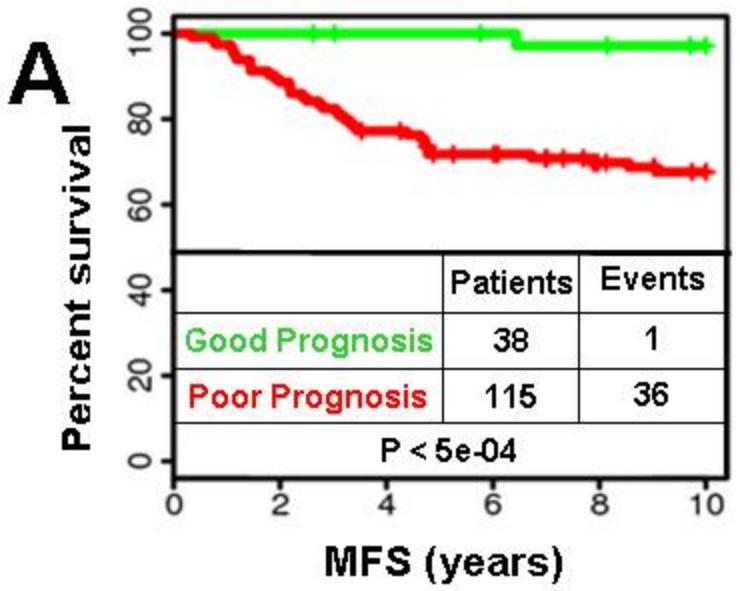

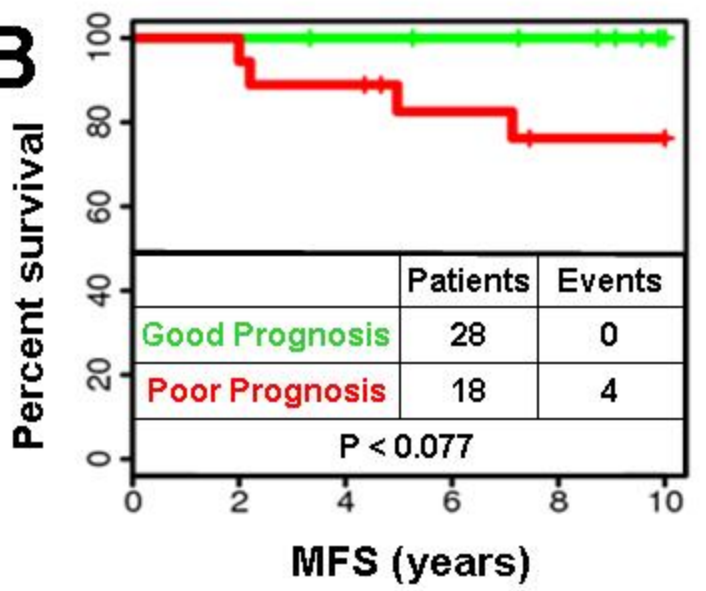

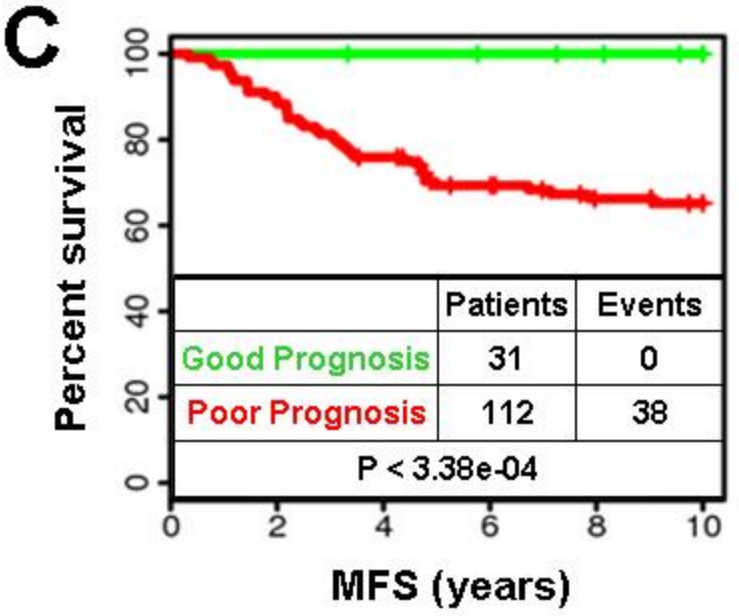

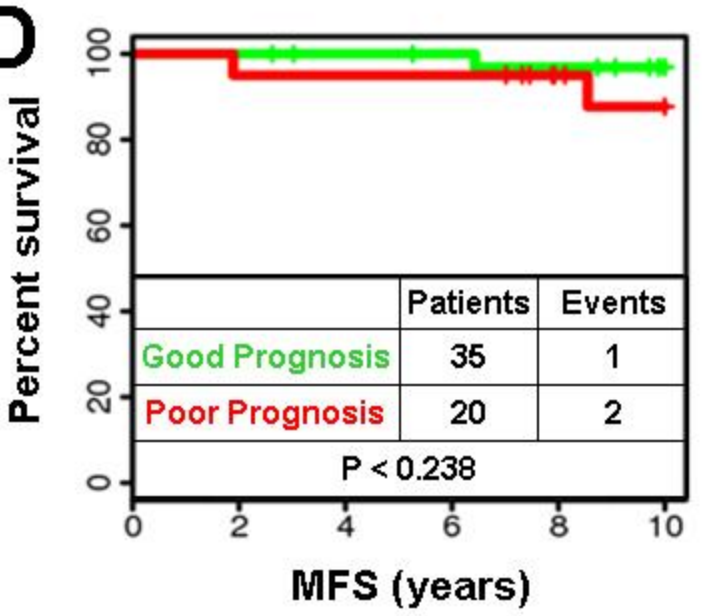

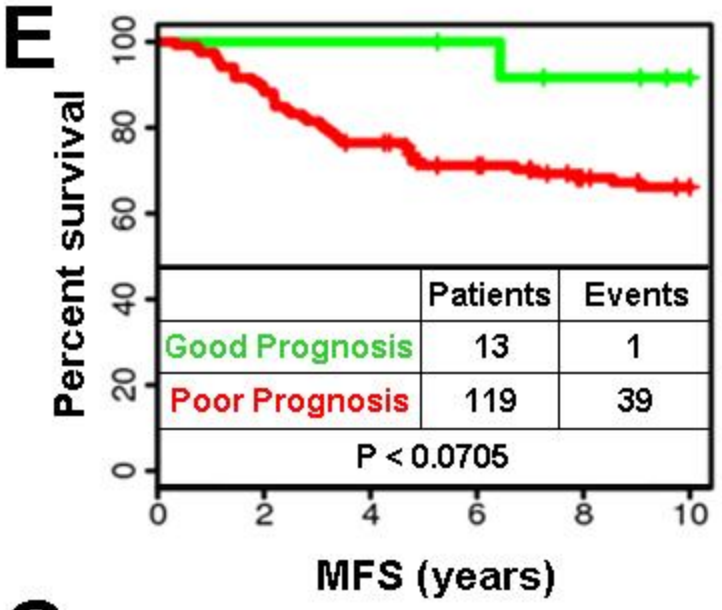

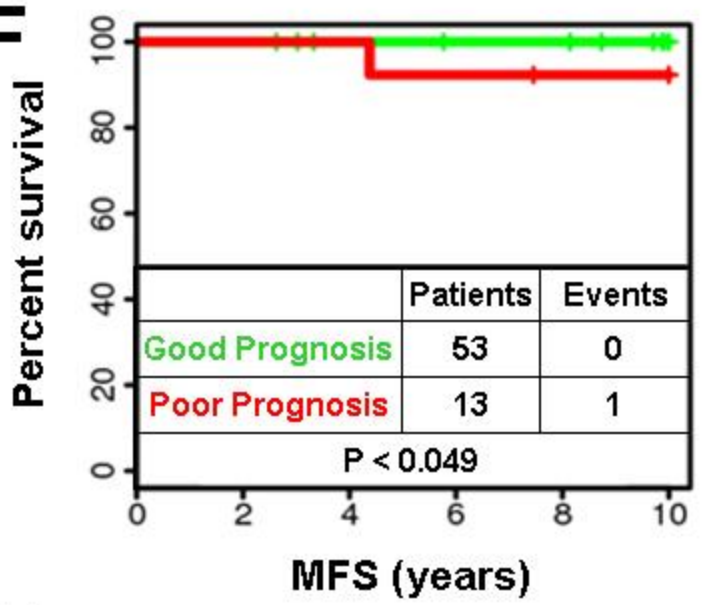

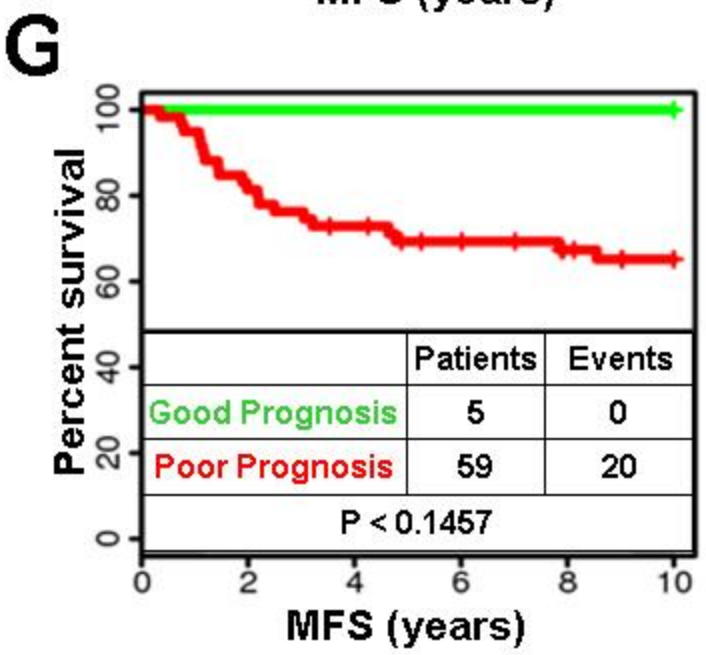

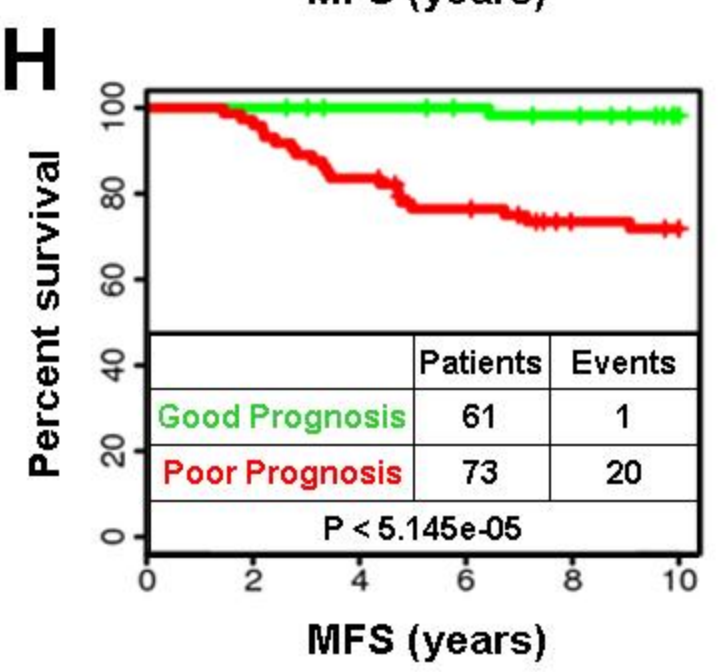

Mira et al., Figure 7

Mira et al., Table 1: Univariate and multivariate Cox regression analyses, comparing the GAB2 signature with existing clinical and genomic predictors in the 198-sample dataset				
Univariate analyses	**p**	**HR**	**lower .95**	**upper .95**
Adjuvant!Online	0,03200	3,09008	1,10129	8,67038
GAB2-Signature	0,00170	23,81942	3,27349	173,32089
Veridex Index	0,00420	5,56595	1,71764	18,03627
MammaPrint	0,00170	23,84934	3,27744	173,54720
Genomic Grade Index	0,00005	5,99948	2,52165	14,27390
Pairwise Multivariate 1	**p**	**HR**	**lower .95**	**upper .95**
GAB2-Signature	0,003	20,947	2,843	154,350
Adjuvant!Online	0,330	1,676	0,593	4,733
Pairwise Multivariate 2	**p**	**HR**	**lower .95**	**upper .95**
GAB2-Signature	0,005	17,65819	2,38999	130,46544
Veridex Index	0,078	2,89930	0,88643	9,48289
Pairwise Multivariate 3	**p**	**HR**	**lower .95**	**upper .95**
GAB2-Signature	0,053	7,91200	0,97100	64,44500
MammaPrint	0,053	7,93600	0,97400	64,64900
Pairwise Multivariate 4	**p**	**HR**	**lower .95**	**upper .95**
GAB2-Signature	0,010	13,66311	1,61679	115,46353
Genomic Grade Index	0,220	1,99342	0,78514	5,06119
Triple Multivariate 1	**p**	**HR**	**lower .95**	**upper .95**
Gab2	0,031	10,510	1,236	89,375
veridex	0,086	2,825	0,864	9,245
Ggi	0,165	1,931	0,762	4,892
Triple Multivariate 2	**p**	**HR**	**lower .95**	**upper .95**
Gab2	0,093	6,725	0,729	62,040
MamPrint	0,079	7,035	0,800	61,859
Ggi	0,626	1,269	0,487	3,310
Triple Multivariate 3	**p**	**HR**	**lower .95**	**upper .95**
Gab2	0,087	6,267	0,766	51,258
MamPrint	0,059	7,501	0,926	60,790
veridex	0,094	2,750	0,842	8,981
Quadruple Multivariate	**p**	**HR**	**lower .95**	**upper .95**
GAB2-Signature	0,140	5,28400	0,57000	49,00400
Veridex Index	0,093	2,75700	0,84400	9,00400
MammaPrint	0,086	6,65800	0,76600	57,88600
Genomic Grade Index	0,610	1,28000	0,49200	3,32900